PRODUCTION OF HIGHER ALCOHOLS FROM ETHANOL OVER LAYERED DOUBLE HYDROXIDES CATALYSTS

Teerud	Panjanapongchai
Prapaipit	Chouykerd
Sunalin	Sutthasathuchana

A SPECIAL PROJECT SUBMITTED IN PARTIAL FULFILLMENT OF
THE REQUIREMENT FOR
THE DEGREE OF BACHELOR OF SCIENCE (INDUSTRIAL CHEMISTRY)
DEPARTMENT OF CHEMISTRY, FACULTY OF SCIENCE
KING MONGKUT'S INSTITUTE OF TECHNOLOGY LADKRABANG
ACADAMIC YEAR 2016

การผลิตแอลกอฮอล์โมเลกุลใหญ่จากเอทานอล โดยใช้ตัวเร่งปฏิกิริยาเลเยอร์ดับเบิลไฮดรอกไซด์

PRODUCTION OF HIGHER ALCOHOLS FROM ETHANOL OVER LAYERED DOUBLE HYDROXIDES CATALYSTS

ธีรุฒมน์ ปัญจนาพงศ์ชัย
ประไพพิศ ช่วยเกิด
สุนลิน สัตถาสาธุชนะ

โครงงานพิเศษนี้เป็นส่วนหนึ่งของการศึกษาตามหลักสูตร
ปริญญาวิทยาศาสตรบัณฑิต (เคมีอุตสาหกรรม)
ภาควิชาเคมี คณะวิทยาศาสตร์
สถาบันเทคโนโลยีพระจอมเกล้าเจ้าคุณทหารลาดกระบัง
ปีการศึกษา 2559

Title Production of higher alcohols from ethanol over layered double hydroxides catalysts
Students Mr. Teerud Panjanapongchai Student ID 56050509
Miss Prapaipit Chouykerd Student ID 56050527
Miss Sunalin Sutthasathuchana Student ID 56050633
Degree Bachelor of science (Industrial Chemistry)
Department Chemistry
Academic Year 2016
Advisor Dr. Natthida Numwong
Co-advisor Assoc. Prof. Dr. Tawan Sooknoi

Faculty of Science, King Mongkut's Institute of Technology Ladkrabang, has approved this special project submitted in partial fulfillment of the requirements for the degree of Bachelor of Science in academic year 2016.

Committees	Signatures
Asst. Prof. Dr. Punnama Siriphannon Chairperson	
Dr. Karoon Sadorn Committee	Karoon Sadorn
Dr. Natthida Numwong Committee and Advisor	Natthida N.
Assoc. Prof. Dr. Tawan Sooknoi Committee and Co-advisor	

Title Production of higher alcohols from ethanol over layered double hydroxides catalysts
Students Mr. Teerud Panjanapongchai Student ID 56050509
Miss Prapaipit Chouykerd Student ID 56050527
Miss Sunalin Sutthasathuchana Student ID 56050633
Degree Bachelor of science (Industrial Chemistry)
Department Chemistry
Faculty Science
University King Mongkut's Institute of Technology Ladkrabang (KMITL)
Academic Year 2016
Advisor Dr. Natthida Numwong
Co-advisor Assoc. Prof. Dr. Tawan Sooknoi

ABSTRACT

In this special project, the conversion of ethanol to higher alcohols was investigated in a continuous fixed-bed reactor using calcined layered double hydroxides (cLDHs) as catalysts. Among LDHs with various Mg/Al ratios (1:1, 2:1, and 6:1), calcined LDHs with Mg/Al ratio 3:1 (cLDHs(3)) give higher yield of higher alcohols. The cLDHs(3) were further modified with metal oxides (Cu-LDHs, Zn-LDHs, and Fe-LDHs) by co-precipitation, Cu-Zn impregnation (Cu-Zn/cLDHs), and Ru adsorption (Ru/cLDHs). It was found that number and strength of acid-basic sites are found to correlate with product selectivity in Guerbet reaction. Zn-cLDHs and Cu-cLDHs show higher activity in promoting the formation of acetaldehyde, as compared to Fe-cLDHs and cLDH(3). Nevertheless, aldol condensation is suppressed by replacing Mg^{2+} with Cu^{2+} and Zn^{2+}. On the other hand, Cu-Zn/cLDHs (4 wt.% Cu-0.8 wt.% Zn and 10 wt.% Cu-2 wt.% Zn) both reduced and non-reduced forms show higher activity for dehydrogenation of ethanol to acetaldehyde, and aldol condensation to high molecular weight products (alcohols and carbonyls), as compared to cLDHs(3). Moreover, lower yield of ethylene, undesired product, was also observed over Cu-Zn/cLDHs. As compared to cLDHs(3), Ru/cLDHs (1 wt.% Ru/LDHs) provide higher ethanol dehydrogenation activity, and also better aldol condensation and hydrogenation activity of the adducts. In addition, lower yield of higher carbonyl compounds was observed over Ru/cLDHs, as compared to Cu-Zn/cLDHs.

Keywords: aldol condensation, ethanol, Guerbet reaction, layered double hydroxides (LDHs), metal oxides.

ACKNOWLEDGEMENTS

For the thesis completion, we would like to gratefully thank our advisor, Dr. Natthida Numwong for her invaluable help, support, supervisions, suggestions and encouragement throughout the thesis. In addition, we sincere thanks our co-advisor, Assoc. Prof. Dr. Tawan Sooknoi for his knowledge and advices.

We would also like to extend our sincere thanks to Assoc. Prof. Dr. Punnama Siriphannon and Dr. Karoon Sadorn for serving as the committee and for their helpful suggestions.

In addition, we are grateful for the supports from Department of Chemistry, Faculty of Science, King Mongkut's Institute of Technology Ladkrabang and Catalytic Chemistry Research Unit for the equipment, chemicals and facilities.

Finally, we would like to express our sincere thank to all teachers, family, friends, laboratory's staffs as well as the member of Catalytic Center Research Unit for their constant guidance advice, valuable supports and encouragement.

Teerud	Panjanapongchai	56050509
Prapaipit	Chouykerd	56050527
Sunalin	Sutthasathuchana	56050633

CONTENTS

CONTENTS (CONTINUED)

CONTENTS (CONTINUED)

LIST OF TABLES

LIST OF SCHEMES

Schemes **Page**

LIST OF FIGURES

CHAPTER 1

INTRODUCTION

1.1 Motivation

Bioethanol is one of the world's most popular renewable resources. One of interesting uses of bioethanol is the conversion of ethanol to higher alcohols such as butanol, hexanol, etc. These higher alcohols can be used as intermediates for value-added chemicals such as medicines, cosmetics, detergents and polyesters [1].

An important reaction to produce higher alcohol from ethanol is "Guerbet reaction". In this reaction, ethanol is adsorbed on the catalyst surface and dehydrogenated to acetaldehyde, follows by aldol condensation of acetaldehydes to a larger unsaturated aldehyde. Final step is hydrogen transfer, which promotes the formation of higher alcohol from unsaturated aldehyde. The reaction mechanism is considered to be on both acidic and basic active sites [2].

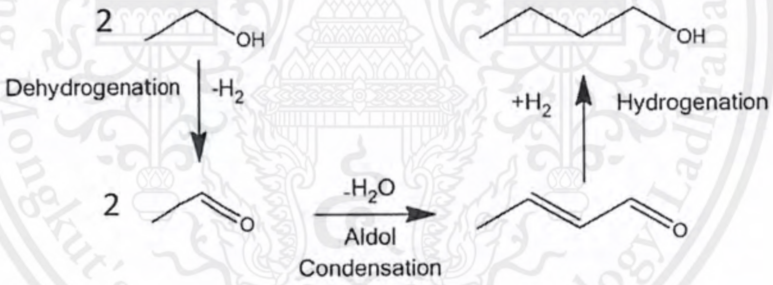

Figure 1.1 Guerbet reaction [3]

Mg-Al mixed oxides is one of the catalyst used for the conversion of ethanol to butanol remarked by many researchers. Layered double hydroxides (LDHs) are materials composed of a lamellar structure of magnesium and aluminum hydroxides. They are a group of clay minerals that have efficiency for various applications such as adsorbents, anion exchangers, additive in polymers, the formation of interesting nano-composite materials, as well as catalysts and precursors to mixed metal oxide catalysts. LDHs are represented by the general formula: $[M^{2+}_{1-x}M^{3+}_{x}(OH)_2]^{x+}[A^{n-}]_{x/n}\cdot mH_2O$, where M^{2+} is divalent cation, such as Mg^{2+}, M^{3+} is a trivalent cation such as Al^{3+} and A^{n-} is an interlayer anion such as CO_3^{2-} and OH^-. LDHs possess both acidic and basic sites. Thus, LDHs are interested to be used as catalyst for the conversion of ethanol to higher alcohols. Thus, LDHs were used as catalyst for the conversion of ethanol to higher alcohols in this special project. The reaction was investigated in a continuous fixed-bed reactor. The effect of incorporated transition metal (Zn, Cu, Fe, Ru) on catalytic activity of LDHs was considered. In addition, the effect of contact time in continuous fixed-bed reactor on product yield and selectivity was also the scope of this special project.

1.2 Objectives

1.2.1. To obtain highly selective and stable catalyst for production of higher alcohols from ethanol.

1.2.2. To obtain optimum reaction conditions: contact time for the conversion of ethanol in continuous fixed-bed reactor.

1.2.3. To understand the effect of Mg/Al ratio of layered double hydroxides (LDHs) on the conversion and selectivity.

1.2.4. To understand the effect of incorporated metal on the catalyst activity, selectivity and stability.

1.2.5. To understand the reaction pathway and mechanism of ethanol conversion to higher alcohols over LDHs catalysts.

1.3 Scopes of study

1.3.1. Prepare LDHs catalysts by co-precipitation and prepare metal incorporated Mg-Al oxides catalysts by co-precipitation, incipient wetness impregnation and adsorption techniques.

1.3.2. Characterize catalyst by X-ray diffraction (XRD), X-ray fluorescence (XRF), nitrogen adsorption (BET), NH3-temperature programmed desorption (NH3-TPD), CO_2-temperature programmed desorption (CO_2-TPD), temperature programmed reduction (TPR) and thermogravimetric analysis (TGA).

1.3.3. Study the conversion of ethanol to higher alcohol in a continuous fixed-bed reactor; contact time (15, 25 and 30 g.h/mol).

1.3.4. Study the effect of Mg/Al ratio and incorporated metal on activity, selectivity and stability of LDHs.

1.3.5. Analyze liquid products by on-line Gas Chromatography with Flame Ionization Detector (GC-FID).

1.4 Expected results

We expect that our study could be an alternative way in improving catalyst with high activity and selectivity for the conversion of ethanol to higher value products in chemical industry.

CHAPTER 2

THEORY AND LITERATURE REVIEWS

2.1 Alcohol

In chemistry, an alcohol is any organic compound in which the hydroxyl functional group functional group (-OH) is bound to a saturated carbon atom. Alcohols are classified into primary, secondary (sec-, s-), and tertiary (tert-, t-), based upon the number of carbon atoms connected to the carbon atom that bears the hydroxyl functional group [4]. In general, the hydroxyl group makes the alcohol molecule polar. Those groups can form hydrogen bonds to one another and to other compounds. Because of hydrogen bonding, alcohols tend to have higher boiling points than comparable hydrocarbons and ethers

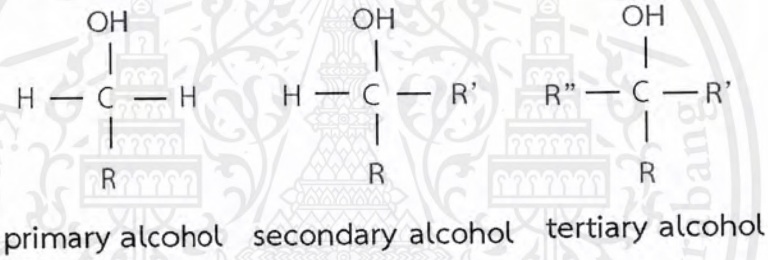

Figure 2.1 The structure of alcohols

Reactions of alcohols can be characterized by cleavage of the O-H bond or the C-O bond either homolytically or ionically. Under normal conditions, alcohols are stable [5]. Alcohols can undergo oxidation to give aldehydes, ketones, or carboxylic acids, or they can be dehydrated to alkenes. They can react to form ester compounds, and they can (if activated first) undergo nucleophilic substitution reactions. The lone pair electrons on the oxygen of the hydroxyl group also make alcohols nucleophiles [6]. Catalytic oxidation or dehydrogenation of primary and secondary alcohols on copper, silver, iron, molybdenum, etc., catalyst leads to the formation of aldehydes and ketones. In the Oppenauer oxidation a secondary alcohol is dehydrogenated by an excess of a ketone [6].

2.2 Ethanol

Ethanol or ethyl alcohol, also called drinking alcohol, is the principal type of alcohol found in alcoholic beverages, produced by the fermentation of sugars by yeasts. It is a neurotoxic psychoactive drug and one of the oldest recreational drugs used by humans. It can cause alcohol intoxication when consumed in sufficient quantity. Its structural formula, CH_3CH_2OH is often abbreviated as C_2H_5OH, C_2H_6O or EtOH [7].

Ethanol melts at −114.1°C, boils at 78.5°C, and has a density of 0.789 g/mL at 20°C. Its low freezing point has made it useful as the fluid in thermometers for temperatures below −40°C, the freezing point of mercury, and for other low-temperature purposes, such as for antifreeze in automobile radiators [8].

The chemical properties of ethanol are dominated by the -OH functional group, which can undergo many industrially important chemical reactions, e.g., dehydration, halogenation, ester formation, and oxidation. Because ethanol can be produced efficiently not only by chemical synthesis from petroleum and coal-based feedstock, but also by fermentation of abundantly available organic materials, its commercial role as a raw material for various chemicals is of increasing importance. Conversion of ethanol to "alkochemicals" is an entirely new approach to producing familiar petrochemicals. Some of these routes are already being used industrially in large alcohol producing countries [9].

2.3 Higher alcohol

2.3.1 Butanol

n-Butanol or n-butyl alcohol or normal butanol is a primary alcohol with a 4-carbon structure and the formula C_4H_9OH. Its isomers include isobutanol, 2-butanol, and tert-butanol. Butanol is one of the group of “fusel alcohol”, which have more than two carbon atoms and have significant solubility in water [10].

Butanol is an alcohol that is produced through petrochemical processes, but can also be produced, like ethanol, through fermentation of sugars derived from corn and agricultural crops. Butanol is a four carbon alcohol; ethanol is a two carbon alcohol. Ethanol is primarily sold as a fuel blend stock for gasoline. N-butanol is sold primarily as a chemical. N-butanol is a superior global chemical with over 8 billion pounds of annual demand in England. Isobutanol is primarily marketed as a fuel blend stock similar to ethanol today and correspondingly has a much lower value as a fuel [11].

2.3.2 Hexanol

1-Hexanol is an organic alcohol with a six-carbon chain and a condensed structural formula of $CH_3(CH_2)_5OH$. This colorless liquid is slightly soluble in water, but miscible with diethyl ether and ethanol. Two additional straight chain isomers of 1-hexanol, 2-hexanol and 3-hexanol, exist, both of which differing by the location of the hydroxyl group. Many isomeric alcohols have the formula $C_6H_{13}OH$. It is used in the perfume industry [12].

2.3.3 Octanol

1-Octanol also known as octan-1-ol is the organic compound with the molecular formula of $CH_3(CH_2)_7OH$. It is a fatty alcohol. Many other isomers are also known generically as octanols. 1-Octanol is manufactured for the synthesis of esters for use in perfumes and flavorings. Esters of octanol, such as octyl acetate, occur as components of essential oils. It is used to evaluate the lipophilicity of pharmaceutical products [13].

2.3.4 Benzyl alcohol

Benzyl alcohol is an aromatic alcohol with the formula $C_6H_5CH_2OH$. It is a colorless liquid with a mild pleasant aromatic odor [14]. It is produced naturally by many plants and is commonly found in fruits and teas. It is also found in a variety of essential oils including jasmine, hyacinth, and ylang-ylang [13]. Benzyl alcohol is used as a general solvent for inks, paints, lacquers, and epoxy resin coatings. Thus, it can be used in paint strippers especially, when combined with compatible viscosity enhancers to encourage the mixture to cling to painted surfaces. It is also a precursor to a variety of esters, used in soap, perfume, and flavor industries. It is also used as a photographic developer [14].

2.4 Aldehyde

Aldehyde, any of a class of organic compounds, in which a carbon atom shares a double bond with an oxygen atom, a single bond with a hydrogen atom, and a single bond with another atom or group of atoms (designated R in general chemical formulas and structure diagrams). The double bond between carbon and oxygen is characteristic of all aldehydes and is known as the carbonyl group. Many aldehydes have pleasant odours, and in principle, they are derived from alcohols by dehydrogenation (removal of hydrogen), from which process came the name "aldehyde".

The only structural difference between hydrocarbons and aldehydes is the presence in the latter of the carbonyl group, and it is this group that is responsible for the differences in properties, both physical and chemical. The differences arise because the carbonyl group is inherently polar—that is, the electrons that make up the C=O bond are drawn closer to the oxygen than to the carbon. This gives the oxygen a partial negative charge and the carbon a partial positive charge [15].

2.4.1 Acetaldehyde

Acetaldehyde is an organic chemical compound with the formula CH_3CHO, sometimes abbreviated by chemists as MeCHO (Me = methyl). It is one of the most important aldehydes, occurring widely in nature and being produced on a large scale in industry. Acetaldehyde occurs naturally in coffee, bread, and ripe fruit, and is produced by plants. It is also produced by the partial oxidation of ethanol by the liver enzyme alcohol dehydrogenase and may be a contributing factor to hangovers from alcohol consumption. Pathways of exposure include air, water, land, or groundwater, as well as drink and smoke. Consumption of disulfiram inhibits acetaldehyde dehydrogenase, the enzyme responsible for the metabolism of acetaldehyde, thereby causing it to build up in the body [16].

2.4.2 Butanal

Butyraldehyde, also known as butanal, is an organic compound with the formula $CH_3(CH_2)_2CHO$. This compound is the aldehyde derivative of butane. It is a colorless flammable liquid with an acrid smell. It is miscible with most organic solvents. Butyraldehyde can be produced by the catalytic dehydrogenation of *n*-butanol. At one time, it was produced industrially by the catalytic hydrogenation of crotonaldehyde, which is derived from acetaldehyde. Upon prolonged exposure to air, butyraldehyde oxidizes to form butyric acid [17].

2.4.3 Hexanal

Hexanal, also called hexanaldehyde or caproaldehyde is an alky aldehyde used in the flavor industry to produce fruity flavors. Its scent resembles freshly cut grass, like cis-3-hexennal [18].

2.4.4 Benzaldehyde

Benzaldehyde (C_6H_5CHO) is an organic compound consisting of a benzene ring with a formyl substituent. It is the simplest aromatic aldehyde and one of the most industrially useful [19]. Benzaldehyde is commonly employed to confer almond flavor to foods and scented products. It is sometimes used in cosmetics product [20].

2.5 Guerbet reaction

Guerbet reaction consists of the following four steps: dehydrogenation of alcohols to the corresponding aldehydes, aldol condensation of the resulting aldehydes, dehydration of the aldol product, and hydrogenation of the unsaturated condensation products to give the higher alcohols as shown in **Figure1.1**. In particular, 1-butanol has been reported to be obtained from ethanol over a variety of solid catalyst, such as alkali earth metal oxides and modified MgO or Mg-Al mixed oxide [21].

Dehydrogenation of alcohols to aldehydes is a typical base-catalyzed reaction, the site requirements for which have been discussed previously for ethanol dehydrogenation reactions, as shown in **Figure 2.2**. Dehydrogenation starts by alcohol chemisorptions on acid-basic site pairs, which cleave O-H bonds to form surface alkoxide intermediates bound to the acid center.

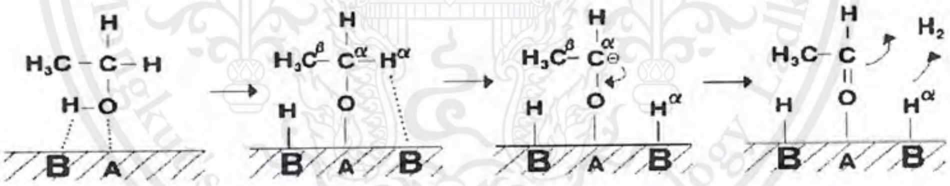

Figure 2.2. Dehydrogenation of alcohols to the corresponding aldehydes [23].

The α-hydrogen in the alkoxide group is then abstracted by a neighboring basic site in order to form adsorbed aldehydes. Aldol condensation reactions on Mg_yAlO_x samples involved also the formation of a carbanion intermediate on Lewis acid-strong Brønsted base pair sites in **Figure2.3**.

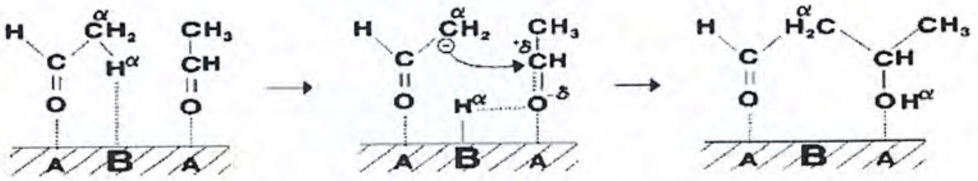

Figure 2.3 Aldol condensation [23].

After aldol condensation, the product of aldol condensation will be dehydrated to crotonaldehyde. Finally, crotonaldehyde will be hydrogenated to 1-butanol in **Figure 2.4.**

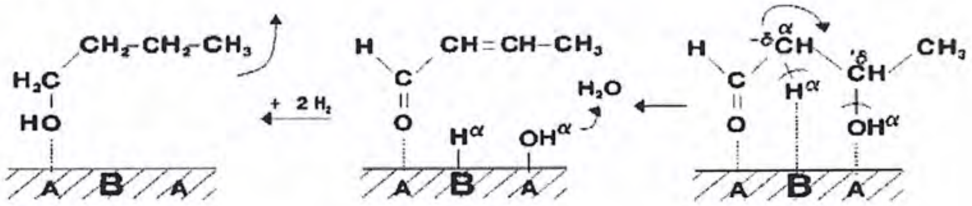

Figure 2.4. Dehydration of the aldol product, and hydrogenation of the unsaturated condensation products [23].

2.6 Catalyst

A catalyst is a substance that speeds up a chemical reaction, but is not consumed by the reaction; hence a catalyst can be recovered. The catalyst is chemically unchanged at the end of the reaction it has been used to speed up, or **catalyze** [24].

Catalytic conversion of ethanol to n-butanol involves the Guerbet reaction, where a primary aliphatic alcohol is converted into its β-alkylated dimer alcohol with loss of one equivalent of water. In 1931, ethanol coupling was first observed on mixtures of MgO, Al_2O_3 and CuO_x. Metal oxides are promising catalysts for ethanol conversion because they give high product selectivities and controllable synthetic processes; for instance, Mg-Al oxide catalysts with different structures show high selectivities for n-butanol in ethanol conversion. Mixed metal oxides catalysts have acid and base sites, which active in aldol condensation reactions [25].

2.6.1 Layered Double Hydroxides (LDHs)

Layered double hydroxides (LDHs) are a group of clay minerals that have shown potential for a number of applications. Some of these include applications as: adsorbents, anion exchangers, medical applications ranging from simple antacids to targeted drug delivery mechanisms, additives in polymers, antiwear addititives in lubricants like motor oil, the formation of interesting nano-composite materials, as well as catalysts and precursors for mixed metal oxide catalysts. LDH are presented by the general formula: $[M^{2+}_{1-x}M^{3+}_{x}(OH)_2]^{x+}[A^{n-}]_{x/n}\cdot mH_2O$

In this formula M^{2+} and M^{3+} represent the divalent and trivalent layer cations respectively, which can be accommodated in the octahedral holes in the brucite-like layers and x is the metal ratio $M^{3+}/(M^{2+}+M^{3+})$. The species A^{n-} in the interlamellar region can be any charge compensating anion (organic or inorganic) and m is the amount of water present in the same region [26].

The hydrotalcite structure results from the stacking of brucite-like layers $[Mg(OH)_2]$ containing a positive residual charge arising from the partial isomerphous substitution of Mg^{2+} cations by Al^{3+} cations. This positive excess charge is balanced by the carbonate anions, which reside in the interlamellar spaces [27] as shown in **Figure 2.5**. It is known that LDHs can collapse to Mg-Al mixed oxides. The calcined LDHs have received increasing attention in the search for environmentally benign catalysts due to their high surface area, acid-base properties, and structure stability, as well as because they can be easily and cheaply synthesized. Therefore, LDHs show potential in catalyze Guerbet reaction for the synthesis of higher alcohols.

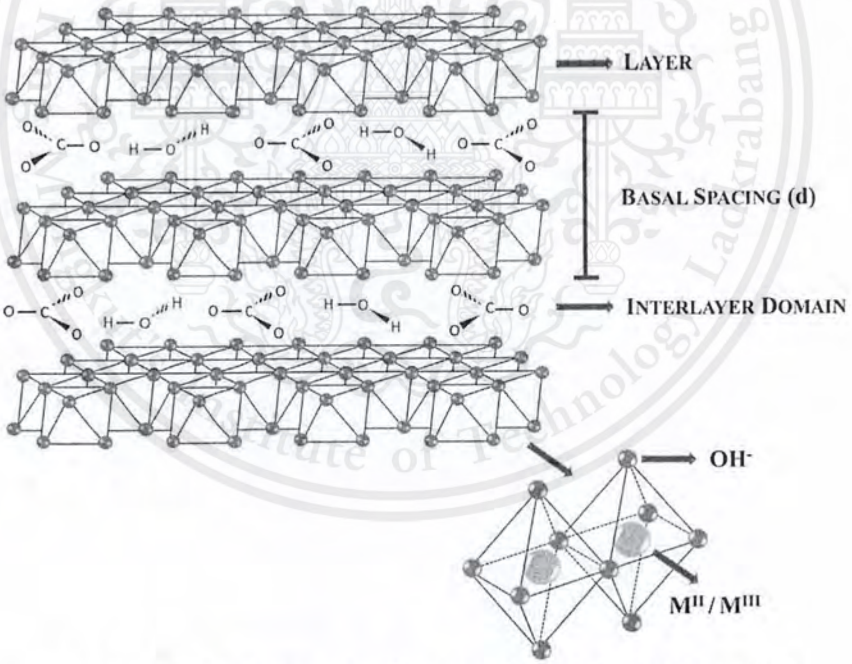

Figure 2.5 The structure of layered double hydroxides [28]

2.7 Literature reviews

Ethanol, a renewable chemical can be converted to higher molecular weight alcohols, so called Guerbet alcohols, to be used for instance, in the production of high-added value solvents and surfactants. The traditional (partly homogeneous) synthesis of Guerbet alcohol is known to proceed via several consecutive steps. Aldehyde formation by alcohol dehydrogenation and its self-aldolization is a well-accepted reaction pathway in the case of the reaction catalyzed by alkali metal hydroxide in the presence of a metallic catalyst [29].

J. I. Di Cosimo, et al. [23] investigated structure, surface, and catalytic properties of Mg-Al basic oxides. Mg-Al mixed oxides with Mg/Al molar ratios of 0.5–9.0 were obtained by thermal decomposition of precipitated hydrotalcite precursors. They studied the effect of incorporation of Al with different Mg/Al molar ratio on aldol condensation of acetaldehyde to 1-butanol. The Mg-Al mixed oxide with Mg/Al 0.47 gives the highest n-butanol product due to acid-based properties on the catalyst surface. They reported the initial adsorption of ethanol on Lewis acid site, and dehydrogenation to ethoxy intermediate, which require acid-strong based pair. In the case of MgO, the isolated O^{2-} ion on MgO surface would be unable to form ethoxide intermediates. Thus, the incorporation of small amounts of Al^{3+} cations to MgO drastically increased the acetaldehyde formation rate because of the generation of new surface Lewis acid–strong base pair sites.

In addition, the effect of composition and surface properties on alcohol-coupling reaction was studied on Mg_yAlO_x catalysts by J.I. Di Cosimo and co-workers . They used ethanol or methanol/propanol mixtures as reactants. They found that rates and product selectivity for ethanol or methanol/propanol reaction strongly depended on the chemical composition of Mg_yAlO_x samples. The rate of alcohol dehydration to ethers and olefins increased with increasing Al content. Al-rich Mg_yAlO_x samples contained a high density of Al^{3+}-O^{2-} site pairs and of moderate strength basic sites, the combination of which promoted the formation of ethylene or propylene from primary alcohols via E2 elimination pathways. The hydrogenation of alcohols to aldehydes (acetaldehyde or propionaldehyde) involved the initial alkoxy intermediate formation on weak Lewis acid-strong Brønsted base site pairs. The results show that the synthesis of acetaldehyde or propionaldehyde was favored on Mg-rich Mg_yAlO_x samples. They found that aldol condensation reactions on Mg_yAlO_x samples involved also the formation of a carbanion intermediate on Lewis acid-strong Brønsted base pair sites and yielded products containing a new C-C bond such as butyraldehyde and isobutyldehyde [23].

M. Leon et al. [21] studied the effect of the total and partial substitution of Al^{3+} by Fe^{3+} on the catalytic performance of hydrotalcite-derived mixed oxides for ethanol condensation reactions. The substitution of Al^{3+} by Fe^{3+} in the structure of the resulting mixed oxide leads to a slight decrease of the basic site and more marked decrease of the concentration of acid site. The almost total abatement of the acid sites of this material largely decreases the selectivity for ethanol dehydration resulting in an increase of the formation of the dehydrogenation product. The substitution of aluminum by iron leads to a crystallinity decrease as in the case of parent hydrotalcites, the crystallinity lose caused by the iron are a consequence of the higher ionic radius of the Fe^{3+} species (67 pm vs 53 pm in the case of the Al^{3+}). Regarding the mixed oxide, MgFeAl presents the highest surface area followed by MgAl, whereas MgFe presents the lowest value.

E.M. Seftel et al. [30] used the co-precipitation at low super saturation method for the synthesis of layered double hydroxides containing Zn^{2+} and Al^{3+} with the cationic ratio of 1-4 and CO_3^{2-} as charge balancing anions. They found that the unit thickness of the interlayer increase with the decrease of the cationic ratio. This observation can be attributed to an increase of the charge density on the brucite-like sheets when the cationic ratio decrease, leading to a higher amount of carbonate anions required to maintain the electro-neutrality of the final material.

B. Dudek et al. [31] presented the impact of an interlayer anion type (carbonate or benzoate) on the structural and textural properties of mixed Mg-Al and Mg-Al-Zn oxide prepared from hydrotalcite, which was prepared by the co-precipitation method. The modification of a carbonate-containing Mg-Al hydrotalcite liked compound with zinc led to significant changes in its thermal stability. A part of carbonate anions in the structure was particularly stable and decomposed at temperatures as high as 600℃. The increase in the zinc content resulted in a weaker carbonates' stabilization and their total decomposition during calcinations.

Y. Zeng et al. [32] successfully synthesized a series of Cu-Mg-Al hydrotalcite-liked compounds with various Cu^{2}/Mg^{2+} molar ratios by hydrothermal crystallization method and used these meterials as catalysts for dehrdrogenation of 2-(1-cyclohexenyl). Hydrotalcite structure, showing that Mg^{2+}cations in the brucite-like layers were substituted by Cu^{2+}cations. After calcinations, the interlayer stack becomes disordered and pores become complex. Coupled with the aggregation, stacking and contraction of oxide phase, so mesopores are formed eventually. Forming a large number of mesopores in the catalyst provides a large open area, good dispersion of copper, so the catalysts exhibit good catalytic activity. It is clear that copper is main active ingredient for dehydrogenation.

I. Marca et al. [33] studied the conversion of ethanol into 1-butanol over Cu-Mg-Al mixed oxide. The optimum yields are obtained for Cu loadings comprised between 5 and 10 wt.%. Effect of the Mg/Al ratio in $Cu_5MgAl_{(y)}O$ sample was studied when the Mg/Al ratio was increased from 1 to 5. It is shown that the effect of Mg/Al ratio does not influence the catalytic activity, and only slightly selectivity. They found that the main pathway is the condensation of ethanol with acetaldehyde resulting in ethyl acetate formation. The strong and the total basicities of the catalysts decrease with increasing the copper content and the selectivity for n-butanol increase when the number of strong basic sites increased.

S. Ching-Yeh et al. [34] studied effect of zinc addition on the copper catalyst activity for the dehydrogenation of isoamyl alcohol. The addition of zinc into copper catalyst can increase its activity as well as its stability. The XRD patterns of the copper catalysts with different zinc loading amounts showed that the peak for zinc oxide is not so apparent, only those of 3% and 5% zinc loading can be observed. This is due to the fact that the addition of zinc results in smaller amounts of crystalline copper on the support. After adding zinc into the copper catalyst, the activities are improved and the deactivation rates are decreased. Apparently, the addition of zinc can not only improve copper dispersion but also provides resistance to the sintering.

L. Dalin et al. [35] investigated methane-carbodioxide (CH_4-CO_2) reforming over Ru supported on Mg and/or Al oxides including γ-Al_2O_3, $MgAl_2O_4$, $Mg_3(Al)O$, and MgO. They found great differences in the Ru metal dispersion and catalytic performance for the CH_4-CO_2 reforming. The characterization results revealed that Ru metal was very highly dispersed on the $Mg_3(Al)O$ mixed oxide obtained from Mg-Al layered double hydroxide, probably existing in very small nanoparticles and/or clusters. The order of Ru metal dispersion was $Ru/Mg_3(Al)O > Ru/MgO > Ru/MgAl_2O_4 > Ru/\gamma$-$Al_2O_3$. The activities of Ru/MgO and $Ru/Mg_3(Al)O$ were higher than those of $Ru/MgAl_2O_4$ and Ru/γ-Al_2O_3, which might be related to the strong base intensity of support and more accessible surface Ru metal atoms, respectively.

L. Seung-Hwan et al. [36] studied the novel types of Ru-based catalysts prepared by solid phase crystallization and impregnation methods in the hydrogenolysis of glycerol under the mild conditions. It showed that hydrotalcite-based catalyst was changed to metal solid solution at 450°C and supported Ru was exposed on the catalyst during calcination. The Ca and Zn modified Ru-based hydrotalcite-like catalyst prepared by solid phase crystallization and impregnation methods showed higher catalytic activity. Ru supported hydrotalcite-based catalysts showed higher acidity and Ru dispersion than Ru/γ-Al_2O_3 catalyst. It was found that the glycerol conversion and selectivity of the 1,2-propanediol in glycerol hydrogenolysis were mainly corresponded to Ru dispersion and the acidity of the catalyst.

CHAPTER 3

EXPERIMENTAL DETAILS

3.1 Reagents

Chemicals	Grade of purity	Manufacturers
1. Ethanol	99.9%	Carlo Erba
2. Nitrogen gas	High purity (99.99%)	Praxair
3. Air	High purity (99.99%)	Praxair
4. Distilled water		
5. Magnesium nitrate hexahydrate [$Mg(NO_3)_2{\cdot}6H_2O$]	98.0%	Panreac
6. Aluminium nitrate nonahydrate [$Al(NO_3)_3{\cdot}9H_2O$]	98.0%	Panreac
7. Copper nitrate trihydrate [$Cu(NO_3)_2{\cdot}3H_2O$]	99.5%	Carlo Erba
8. Zinc nitrate hexahydrate [$Zn(NO_3)_2{\cdot}6H_2O$]	97.5%	Carlo Erba
9. Iron nitrate nonahydrate [$Fe(NO_3)_3{\cdot}9H_2O$]	98.5%	QReC
10. Sodium hydroxide [$NaOH$]	98%	Carlo Erba
11. Sodium Carbonate [Na_2CO_3]	99.5%	Carlo Erba
12. Dichloro (p-cymene) ruthenium(II) dimer	-	Sigma-Aldrich
13. Toluene	99.5%	Lab-Scan
14. Acetone	99.8%	QReC

3.2 Apparatus

1. Syringe (10 mL)
2. Syringe pump
3. Magnetic stirrer
4. pH meter
5. Laboratory glassware
6. Laboratory plastic ware
7. Oven
8. Furnace
9. Sieve
10. Catalytic testing rig
11. Mass flow controller
12. Temperature programmed desorption (TPD) system
13. Temperature programmed reduction (TPR) system
14. X-ray fluorescence spectrometer (Wavelength Dispersive, Philips, PW2400, Scientific and Technological Research Equipment Centre 2-3 Building, Chulalongkorn University and Energy Dispersive, Oxford, ED-2000, Scientific and Technological Research Equipment Centre 2-3 Building, Chulalongkorn University)
15. X-ray powder diffractometer (Rigaku, DMAX 2200/Ultima+, Faculty of Science, Chulalongkorn University)
16. Thermogravimetric analyzer (Perkin-Elmer, Scientific Instrument Service Centre, KMITL)
17. Gas Chromatography with flame ionization detector (GC-FID)
18. Gas Chromatography-mass spectrometer (GC-MS) (Agilent Technologies, 6890N Network GC system)

3.3 Experimental procedure

3.3.1 Catalyst preparation

3.3.1.1 Preparation of LDHs catalysts

The LDHs catalysts were prepared by co-precipitation method. The aqueous solution of 1 M $Mg(NO_3)_2{\cdot}6H_2O$ and 1 M $Al(NO_3)_3{\cdot}9H_2O$ containing required Mg/Al ratio (1:1, 2:1, 3:1, and 6:1 molar ratio) were prepared. This solution was contacted with a basic solution by drop-wise addition of both solutions into a 0.5 M Na_2CO_3, and maintaining pH at 10 by 3.4 M NaOH solution. Afterwards, the mixture was aged at 65°C for 18 h under vigorous stirring. Then the precipitate was washed several times with distilled water, and dried at 110°C in the air overnight. The obtained solid was ground into a powder and calcined at 450°C for 4 h under air (60 mL/min) with a heating rate of 1°C/min and the LDHs-derived Mg-Al mixed oxides was obtained [39].

3.3.1.2 Preparation of transition metal/Mg/Al mixed oxides catalysts

Transition metal/Mg/Al mixed oxides were synthesized by using the same technique as for LDHs by partial substitution of Mg^{2+} and Al^{3+} with divalent cation (Zn^{2+} and Cu^{2+}) and trivalent cation (Fe^{3+}), respectively. The molar ratios of M^{2+}/M^{3+} was controlled at constant value. The precursors for Zn, Cu, and Fe were $Zn(NO_3)_2{\cdot}6H_2O$, $Cu(NO_3)_2{\cdot}3H_2O$, and $Fe(NO_3)_3{\cdot}9H_2O$, respectively.

3.3.1.3 Preparation of 4 wt.% Cu-0.8 wt.% Zn supported cLDHs (Mg/Al ratio 3:1)

Before adsorption, the LDHs (Mg/Al ratio 3:1) supports were calcined at 450°C for 4 h under air (60 mL/min) with a heating rate of 1°C/min in order to remove adsorbed water on the surface. The 1 M Cu and 1 M Zn precursor solutions were prepared by dissolving 0.8066 g of $Cu(NO_3)_2{\cdot}3H_2O$ and 0.1929 g of $Zn(NO_3)_2{\cdot}6H_2O$ in DI water, respectively. After that, 5.7456 g of cLDHs was impregnated with the Cu and Zn precursor solutions in plastic beaker. The mixture was gradually dried in an oven at 80 °C to remove excess water until the catalyst was almost dried. Then, it was calcined in tube furnance at 450°C for 4 h under air (60 mL/min) with a heating rate of 1°C/min to obtain CuO and ZnO. After that, CuO and ZnO were reduced at 10°C/min to 400°C for 3 h under hydrogen (30 mL/min) in a reactor to obtain CuZn alloy form.

3.3.1.4 Preparation of 10 wt.% Cu-2 wt.% Zn supported cLDH (Mg/Al ratio 3:1)

Before adsorption, the LDHs (Mg/Al ratio 3:1) supports were calcined at 450°C for 4 h under air (60 mL/min) with a heating rate of 1°C/min in order to remove adsorbed water on the surface. The 1 M Cu and 1 M Zn precursor solutions were prepared by dissolving 1.9024 of $Cu(NO_3)_2 \cdot 3H_2O$ and 0.4550 of $Zn(NO_3)_2 \cdot 6H_2O$ in DI water, respectively. After that, 4.4000 g cLDHs was impregnated with the Cu and Zn precursor solutions in plastic beaker. The mixture was gradually dried in an oven at 80 °C to remove excess water until the catalyst was almost dried. Then, it was calcined in tube furnance at 450°C for 4 h under air (60 mL/min) with a heating rate of 1°C/min to obtain CuO and ZnO. After that, CuO and ZnO were reduced at 10°C/min to 400°C for 3 h under hydrogen (30 mL/min) in a reactor to obtain CuZn alloy form.

3.3.1.5 Preparation of Ru adsorbed cLDHs (Mg/Al ratio 3:1)

Before adsorption, the LDHs (Mg/Al ratio 3:1) supports were calcined at 450°C for 4 h under air (60 mL/min) with a heating rate of 1°C/min in order to remove adsorbed water on the surface. The 1 M Ru precursor solution was prepared by dissolving 0.2424 g of Dichloro (p-cymene) ruthenium(II) dimer in toluene and acetone. After that, 2.7576 g of cLDHs was adsorbed with the Ru precursor solution until yellow solution changed to orange under vigorous stirring. Then the precipitate was washed several times with toluene, and dried at 110°C in the air overnight to remove excess water until the catalyst was almost dried. Then, it was calcined in tube furnance at 450°C for 4 h under air (60 mL/min) with a heating rate of 1°C/min to obtain RuO. After that, RuO was reduced at 10°C/min to 400°C for 3 h under hydrogen (30 mL/min) in a reactor to obtain Ru metal form.

3.3.2 Catalyst characterization

3.3.2.1 Structural analysis using X-ray diffraction (XRD)

The crystalline phase of the prepared materials can be identified using XRD measurement. The sample was ground before it is packed on the sample holder. Analysis was done employing Rigaku diffractometer (Cu-Kα radiation, 40 kV, 30 mA), covering the range of 2θ = 10-70°, at the rate of 0.02°/step, and a scanning rate of 1 s/step.

3.3.2.2 Quantitative elemental composition analysis by X-ray fluorescence (XRF)

X-ray fluorescence is a surface composition determination that results from bombarding the sample with high-energy X-rays to releases characteristic secondary X-ray. This technique can be performed according to the procedure: the 0.5 g of catalyst sample and 4.5 g of boric acid were mixed, ground together, and compressed into an alumina pan before bring into the XRF sample holder in XRF instrument.

3.3.2.3 Determination of specific surface area by nitrogen adsorption

Surface area of the catalysts can be determined by a gas adsorption analyzer (Autosorb-1C, Quantachrome). Approximately 0.0800 g of the sample was loaded into the cell, which was attached to the outgassing station equipped with a heating mantle. The temperature was raised to 350°C during outgassing process. After that, nitrogen gas was introduced to the sample cell where the adsorption can be measured at the range of the partial pressure (P/P_0) from 10^{-6} to 1.0. The adsorption isotherm and the corresponding surface area were analyzed using ***BET equation*** as shown in **Equation 3.1**.

$$\frac{1}{\upsilon\,[(p_0/p)-1]} = \frac{c-1}{\upsilon_m c}\left(\frac{p}{p_0}\right) + \frac{1}{\upsilon_m c} \qquad \text{Equation 3.1}$$

Where p and p_0 are the equilibrium and the saturation pressure of adsorbents at the temperature of adsorption, υ is the adsorbed gas quantity (for example, in volume units), υ_m is the monolayer adsorbed gas quantity, and C is the BET constant. The concept of the theory is an extension of the Langmuir theory, which is a theory for monolayer molecular adsorption to multilayer adsorption with the following hypotheses: (a) gas molecules physically adsorb on a solid in layers infinitely; (b) there is no interaction between each adsorption layer; and (c) the Langmuir theory can be applied to each layer.

3.3.2.4 Determination of acidity of the catalysts by NH_3-temperature programmed desorption (NH_3-TPD)

The acid function of the catalyst was identified using NH_3-TPD measurement. Samples (0.2 g) was preheated in flowing air zero at 450°C for 2 h and evacuated and then it was exposed to 20 kPa of 1% NH_3/He gas at 31°C until saturation coverage was reached. After the sample will be flushed with He at room temperature for 1 h, the temperature was then increased at a linear rate of 10°C/min from 50 to 850°C under vacuum. The TPD spectra was normalized based on the specific surface area.

3.3.2.5 Determination of basicity of the catalyst by CO_2-temperature programmed desorption (CO_2-TPD)

The basic function of the catalyst was identified using CO_2-TPD measurement. Samples (0.2 g) was preheated in the flowing of air zero at 450°C for 2 h and evacuated and then it was exposed to 20 kPa of pure CO_2 gas at 31°C until saturation coverage was reached. After that, the sample was flushed with He at room temperature for 1 h, the temperature was then increased at a linear rate of 10°C/min from 50 to 850°C under vacuum. The TPD spectra was normalized based on the specific surface area.

3.3.2.6 Determinationof thermal stability of thermogravimetric analysis (TGA)

Phase transformation upon the heating treatment is a convenient method to study thermal stability. The samples were manually grinded in mortar to homogeneous fine particles for a while, then 10 mg of the samples was weighed approximately into platinum pan to perform on thermogravimetric analysis (Pyris) in 20 mL/min of nitrogen atmosphere. The temperature was scanned from 50 to 900°C with heating rate of 10°C/min. The data was collected corresponding to mass loss during the temperature range.

3.3.2.7 Determination of metal reduction temperature of the catalysts by temperature programmed reduction (TPR)

Temperature-programmed reduction (TPR) provides information on the active site species of the catalysts by monitoring their reducibility. Temperature programmed reduction was measured using thermal conductivity detector (TCD). The sample weighed 0.2 g was placed into a quartz tube reactor, which will be located inside a temperature-regulated furnace. Prior to the H_2-TPR, each sample was heated to its activations temperature 400°C in air zero (30 mL/min) for 2 h with 10°C/min and was cooled down to below 50°C. The heating rate of 10°C/min and 30 mL/min of 10% H_2 in Ar was applied for TPR analysis. Water production during the reduction process was removed in a U-shape glass trap at -95 °C (vapor of liquid N_2) before entering the TCD.

3.3.3 Catalytic activity testing

Catalytic conversion of ethanol was carried out at 380°C using 0.3 g of catalyst in a fixed-bed continuous-flow glass reactor (8 mm). The catalyst powders were pelletized and crushed to the desired size (600-850 μm). After that, it was packed into a glass tube reactor and covered with glass wool and glass beads. The reactor was located at the center of a vertical tube furnace. Nitrogen was used as carrier gas. Gas flow rate was controlled by a mass flow controller and was checked by a bubble flow meter. The scheme of catalytic testing rig is shown in **Figure 3.1**. Before the catalytic reaction, the as-prepared catalysts were pretreated at 400°C for 1 h in air zero flow (30 mL/min). Ethanol was introduced into the reactor using a syringe pump at 0.7 mL/h. The catalytic testing was conducted for a total time on stream (TOS) of 6 h. The product effluents were analyzed online through a gas chromatograph, previously calibrated for the reaction products response.

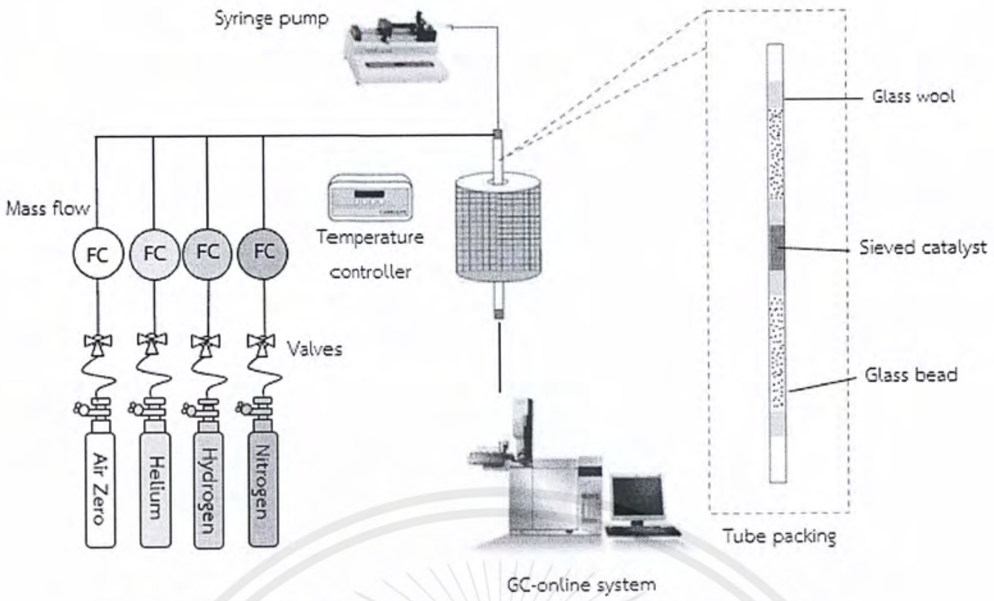

Figure 3.1 Catalytic activity testing rig

3.3.4 Products analysis

The products identification was confirmed by online gas chromatograph equipped with a flame ionized detector (GC–FID, CP-3800). The products were collected in a gas sampling loop, and then periodically injected into GC column with an inert carrier nitrogen gas. The temperature of the injection port was set at 200°C, 35°C for column oven, and 250°C for FID detector. The GC temperature condition was started at 35 °C, hold for 2 min then heated up to 200 °C. Pressure of the carrier gas was fixed to 14 psi all time. The products were recorded as a chromatogram. Each peak areas from the chromatogram was measured and calculated. Compared with standard peak areas, the species and composition of each product was determined.

CHAPTER 4

RESULTS AND DISCUSSION

4.1 Catalyst characterization

4.1.1 X-Ray Powder Diffraction (XRD)

Figure 4.1 shows the XRD patterns of LDHs before and after calcination. Regarding to the XRD pattern of the non-calcined LDHs Mg/Al ratio 3:1, it reveals sharp and symmetric peaks for (003), (006), (110) and (113) planes, as well as broad symmetric peaks for (009), (015) and (016) planes, which are characteristic of a lamellar material [37].

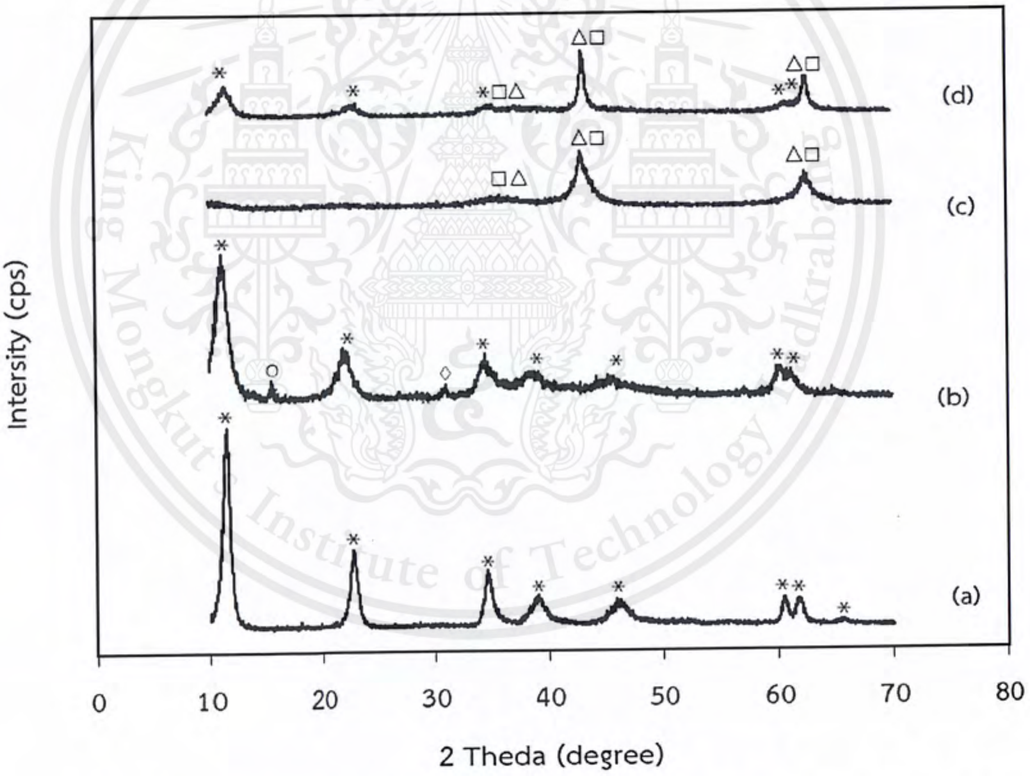

Figure 4.1 XRD patterns of non-calcined LDHs Mg/Al ratio (a) 3:1, (b) 6:1 and calcined LDHs Mg/Al ratio (c) 3:1, (d) 6:1 (under a flow of air zero at 450°C for 4 h): (*) LDHs, (△) MgO, (□) MgO-Al_2O_3, (O) AlO(OH) (boehmite) and (◇) $MgCO_3$

After calcined at 450°C, the layered structure of LDHs was completely collapsed. Only broad peaks of MgO-Al_2O_3 and MgO phases were observed as shown in **Figure 4.1(c)** [38,39]. No aluminium oxide phase was detected, suggesting that aluminium oxides are either well dispersed or forming an amorphous phase. However, the XRD pattern of Mg/Al ratio 6:1 (**Figure 4.1(b) and (d)**) show the presence of AlO(OH) (boehmite) and $MgCO_3$ as an impurity phases [40], suggesting that the crystal of LDHs(6) is not complete. Calcined LDHs(6) still has MgO-Al_2O_3 and MgO, which remain in LDHs phase. This is because calcined LDHs can recrystallize to LDHs by adsorbing water from moisture.

4.1.2 Elemental composition, surface area, acid and basic characteristics of catalysts

The elemental composition, specific surface area, acidity, and basicity of the catalysts were determined by X-ray fluorescence (XRF), BET measurement and temperature programmed desorption (TPD), respectively. The results are shown in **Table 4.1**.

Table 4.1 Elemental composition, surface area, acid, and basic characteristics of catalysts

Catalysts	Elemental composition (wt.%)			M^{2+}/M^{3+}	Surface area (m^2/g)	Acidity (mmol /g)	Basicity (mmol /g)
	Mg	Al	Metal				
cLDHs(1)	-	-	-	1	188	8.2	41.0
cLDHs(2)	-	-	-	2	233	11.8	54.1
cLDHs(3)	49.1	18.6	-	3	189	5.1	76.2
cLDHs(6)	-	-	-	6	158	2.9	47.5
Cu-cLDHs(a) (Cu:Mg:Al=0.4:2.6:1)	22.5	14.2	14.2(d)	3	134	5.4	52.2
Zn-cLDHs(a) (Zn:Mg:Al=0.4:2.6:1)	24.8	10.8	-	3	263	5.1	35.8
Fe-cLDHs(a) (Mg:Al:Fe=3:0.5:0.5)	-	-	-	3	185	6.1	51.1
1 wt.% Ru/cLDHs(b)	-	-	1.8(e)	3	323	10.0	51.8
4 wt.% Cu-0.8 wt.% Zn /cLDHs(c)	27.8	9.58	3.3(d) 0.7(f)	3	300	5.1	62.4
10 wt.% Cu-2 wt.% Zn /cLDHs(c)	-	-	-	3	170	9.7	68.0

(a) prepared by co-precipitation

(b) prepared by adsorption

(c) prepared by impregnation

(d) Cu

(e) Ru

(f) Zn

As shown in **Table 4.1**, the calcined LDHs possess both acid and basic properties, due to the presence of Mg-O pair (basic site) and Al^{3+} (acid site) in the structure. **Table 4.1** presents that increasing the Mg/Al ratio leads to an increase in the number of basic sites and a decrease in the number of acid sites except cLDHs(6) because of incomplete crystal, as shown in **Figure4.1(b)**. However, the number of acid and basic sites are slightly decreased when LDHs was incorporated with other metal oxides. This may be because these acid and basic sites are obscured by the incorporated species. Moreover, it is also found that surface areas of these metal oxide incorporated LDHs remain almost the same as the parent LDHs. This is because only small amount of metals are loaded (co-precipitation method). The adsorption of Ru on cLDHs(3) leads to a decrease in strong acid sites as observed by **Figure 4.2(c)**, suggesting that Ru interact with Al^{3+} on the cLDHs surface. The 4 wt.% Cu-0.8 wt.% Zn alloy/cLDHs(3) catalyst has similar amount acid site of cLDHs(3) but the 10 wt.% Cu-2 wt.% Zn alloy/cLDHs(3) catalyst has acidity higher than that of cLDHs(3). Because Zn is good Lewis acid lead to a increase in strong acidity of the 10 wt.% Cu-2 wt.% Zn alloy/cLDHs catalyst as shown by **Figure 4.2(c)**.

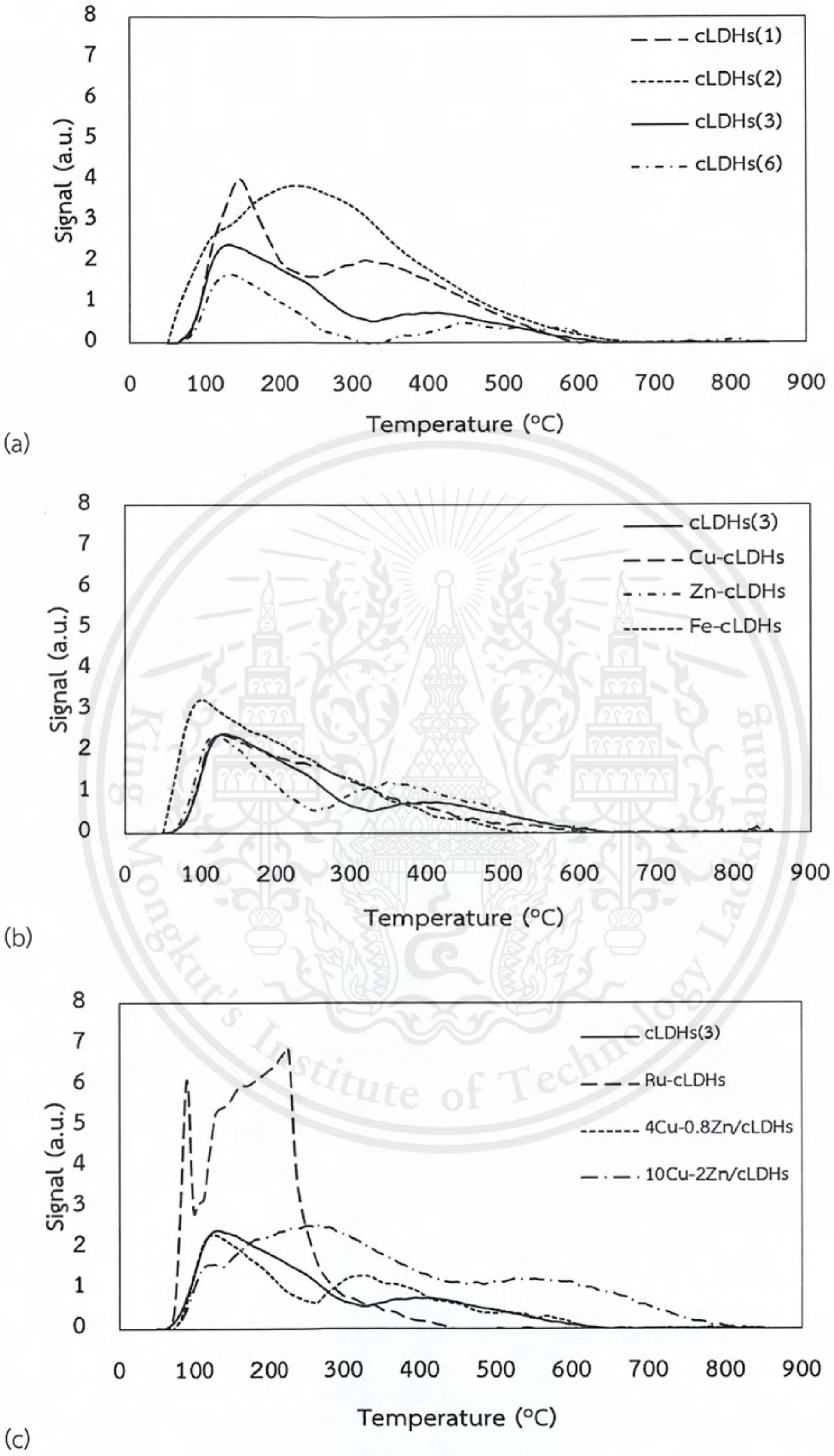

Figure 4.2 NH_3-temperature programmed desorption profile of catalysts

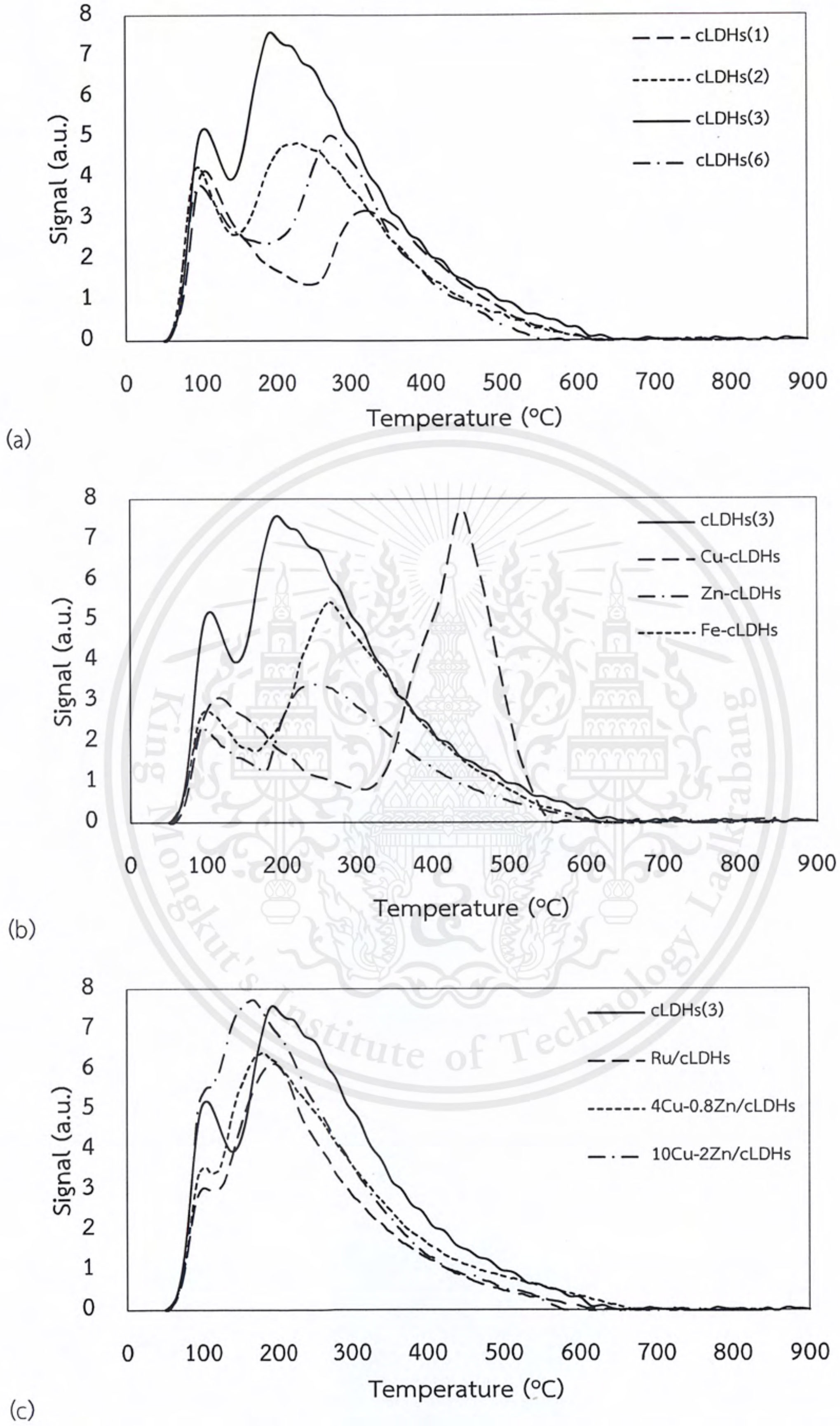

Figure 4.3 CO_2-temperature programmed desorption profile of catalysts

4.1.3 Thermogravimetric Analysis (TGA)

Figure 4.4 shows TGA result of the as-prepared LDHs (Mg/Al ratio 3:1). The first weight loss below 180°C is associated with the evaporation of adsorbed and intercalated water molecules.

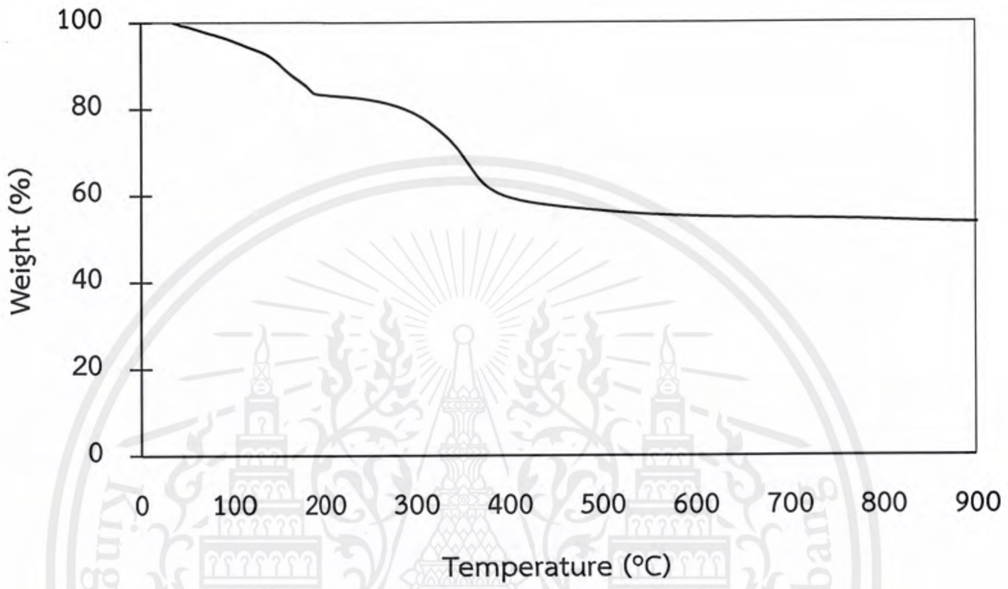

Figure 4.4 TGA analysis (under air) of non-calcined LDHs Mg/Al ratio 3:1

Another step of weight loss between 180°C and 400°C referred to the decomposition of the interlayer between carbonate and hydroxyl groups in the lamellae structure of the LDHs leading to collapse of the layer structure [38], which is consistent with the result of calcined-LDHs obtained from XRD (**Figure 4.1(b)**).

4.1.4 Temperature program reduction characteristics (TPR)

As shown in **Figure 4.5**, Ru/cLDH(3) catalyst shows two reduction peaks at 130°C and 170°C, which are attributed to the reduction of well-dispersed RuO_x species and bulk RuO_2 species, respectively [35].

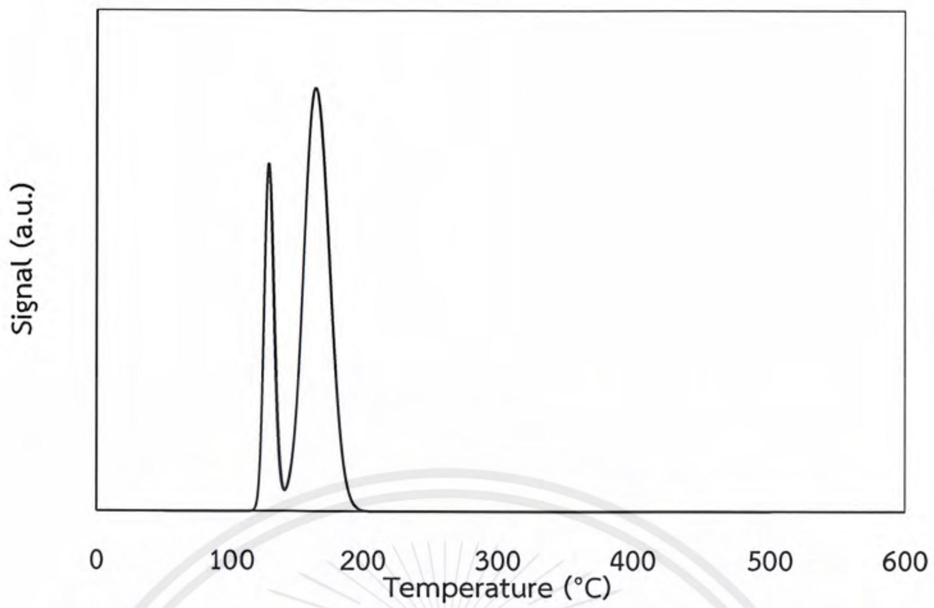

Figure 4.5 TPR profiles of adsorption 1 wt.% Ru/cLDHs catalyst *(10% H_2/Ar, ramping at 10°C/min)*

As shown in **Figure 4.6** (a), pure copper catalyst shows only single reduction peak at 280°C, attributed to the reduction of CuO to metallic Cu [32]. In the case of 4 wt.% Cu-0.8 wt.% Zn alloy/cLDHs catalyst, these is no reduction peak observed suggesting that zinc may reduce copper during calcination. Reduction of ZnO cannot be evidenced [34]. While 10 wt.% Cu-2 wt.% Zn alloy/cLDHs catalyst shows a reduction peak at low temperature, which is attributed to the reduction of CuO and ZnO to CuZn alloy. Hence, adding zinc into the copper catalyst leads to the shift of reduction peak to lower temperature, as compared to the pure copper catalyst. It is suggested that zinc may well modify the copper dispersion and the interaction between copper and support, which cause copper oxide to reduce more easily.

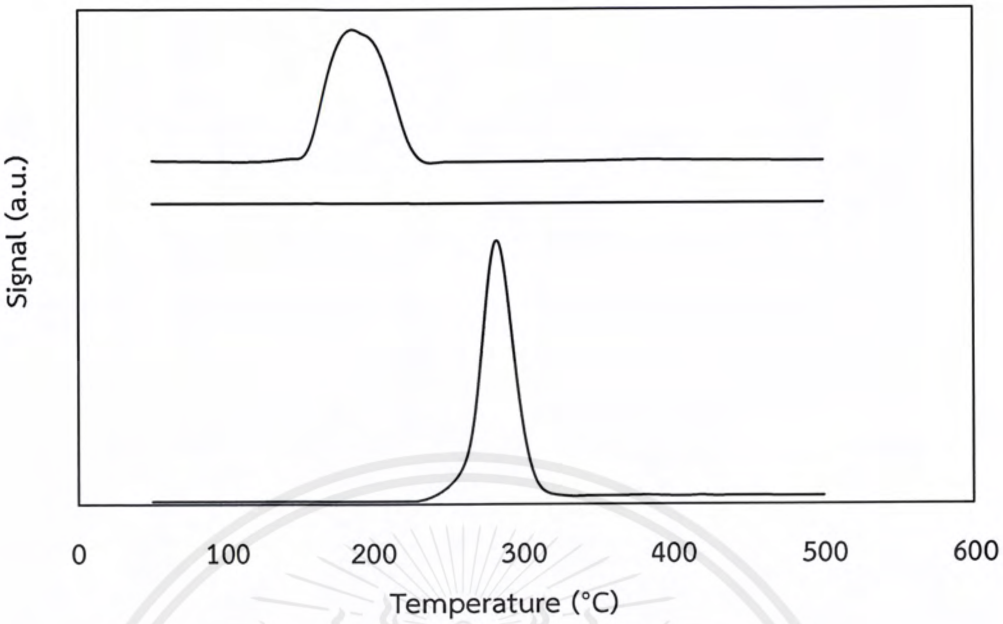

Figure 4.6 TPR profiles of (a) pure copper, (b) impregnation 4 wt.% Cu-0.8 wt. % Zn alloy/cLDHs and (c) impregnation 10 wt.% Cu-2 wt.% Zn alloy/cLDHs catalysts *(10% H_2/Ar, ramping at 10°C/min)*

4.2 Conversion of ethanol to higher alcohols

4.2.1 Effect of Mg/Al ratio

In order to study the effect of acid and basic sites, the conversion of ethanol over LDHs catalysts with various Mg/Al molar ratios (1:1, 2:1, 3:1 and 6:1) prepared by co-precipitation method were primarily investigated under the same reaction conditions in a fixed-bed reactor (380°C, 1 atm, 60 mL/min N_2 carrier gas, 25 g.h/mol contact time). It can be seen that the conversion is steady over 360 min on stream, suggesting no deactivation of the catalysts.

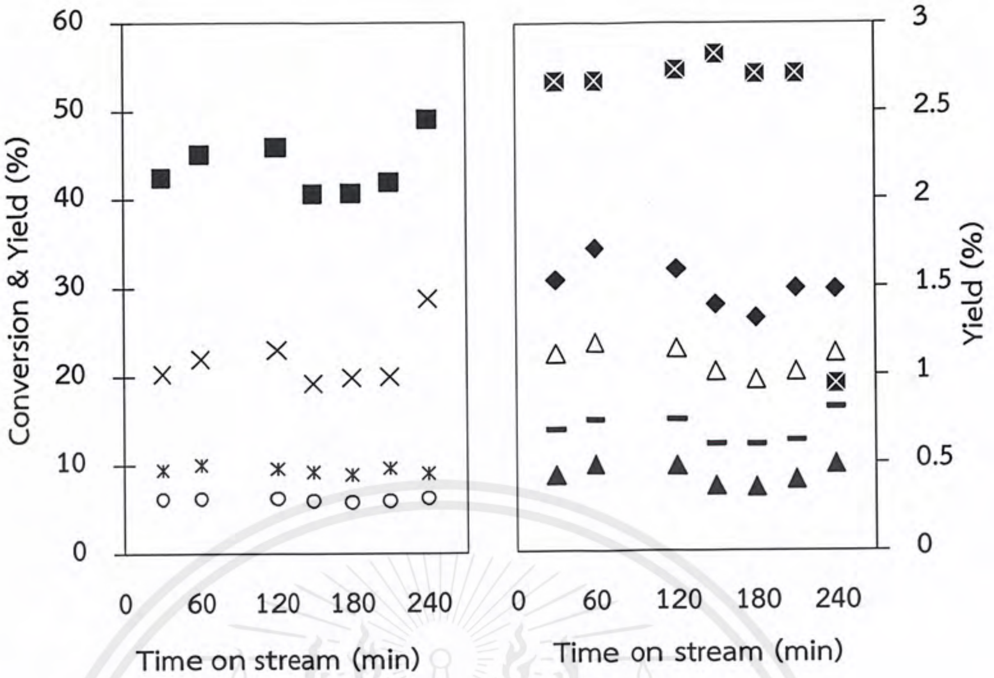

Figure 4.7 Conversion of ethanol and yields of major products (a) and minor products (b) over cLDHs(3). *(Reaction condition; temperature: 380°C, pressure: 1 atm, contact time: 25 g.h/mol, flow rate of N_2 carrier gas: 60 mL/min, results at 4 hours of time on stream)*

■ Conversion, × Ethylene, ✱ C4 alcohols, ○ Acetaldehyde, ☒ Diethyl ether, ▬ Acetone , △ Butanal, ☐ Diethyl acetal, ◆ C6 alcohols, ▲ C7 carbonyls

Table 4.2 presents the product distribution of various catalysts. It can be seen that, cLDHs with Mg/Al ratio 1:1, 2:1, 3:1, and 6:1 provide in an ethanol conversion ~40-50%. Increasing Mg content of cLDHs remarkably gives higher yield of C4 alcohols and 2-ethyl-1-butanol. This is because increasing the Mg ratio would provide higher amount of basic sites that promotes dehydrogenation of ethanol and condensation of acetaldehyde. These results are confirmed by CO_2-TPD that high Mg content shows higher amount of basicity. However, the cLDHs(6) which contains higher amount of Mg gives lower yield of aldehyde, a dehydrogenation product from ethanol. This is due to the lower density of strong basic sites as confirmed by TPD results (**Figure 4.3(a)**).

Table 4.2 Conversion of ethanol and products yield over cLDHs catalysts with different Mg/Al ratio.

Catalysts	**cLDHs(1)**	**cLDHs(2)**	**cLDHs(3)**	**cLDHs(6)**
Conversion (%)	39.3	50.9	43.7	49.1
Yield of Product (%)				
Ethylene	31.0	32.3	21.9	29.3
Diethyl ether	0.5	0.8	2.5	4.5
Acetaldehyde	4.9	6.0	6.1	5.4
Acetone	1.1	0.7	0.7	0.7
Butanal	0.7	1.0	1.1	0.8
Diethyl acetal	-	0.3	-	0.2
Isobutylaldehyde dimethyl acetal	-	-	-	-
C4 alcohols[a]	5.9	8.3	9.4	7.1
C6 alcohols[b]	0.4	1.1	1.5	0.8
C7 alcohols[c]	-	-	-	-
C8 alcohols[d]	-	-	-	-
Aromatic alcohols[e]	-	-	-	-
C5 carbonyls[f]	-	-	-	-
C6 carbonyls[g]	-	-	-	-
C7 carbonyls[h]	0.5	0.4	0.4	0.2
C8 carbonyls[i]	-	-	-	-
C9 carbonyls[j]	-	-	-	-
Aromatic carbonyls[k]	-	0.1	-	0.1
Unknown	-	-	-	-

(a) : 1-Butanol and 2-Butenol

(b) : 2-Ethyl-1-butanol, 1-Hexanol and 3-Hexen-1-ol

(c) : 2,4-Dimethyl-2-pentanol

(d) : 2-Ethyl-1-hexanol and Octanol

(e) : Benzyl alcohol and 3,5-Diethylphenol
(f) : 2-Pentanone
(g) : Hexanal
(h) : 4-Heptanone and 3-Methylcyclohexanone
(i) : 2-Ethylhexanal and 2-Ethylcyclohexanone
(j) : 4-nonanone and 2-Ethylcyclohexanone
(k) : Benzaldehyde, 3-Methylbenzaldehyde, 4-Methylbenzaldehyde, Acetophenone, 1-Phenyl-1-butanol and 4-Ethylacetophenone

(Reaction condition; temperature: 380°C, pressure: 1 atm, contact time: 25 g.h/mol, flow rate of N_2 *carrier gas: 60 mL/min, average result from 6 h of time on stream)*

In line with this view, the yield of dehydrogenation and aldol products depend on basicity of the catalysts as shown in **Figure 4.8**. This is because dehydrogenation of ethanol is a typical base-catalyzed reaction [17].

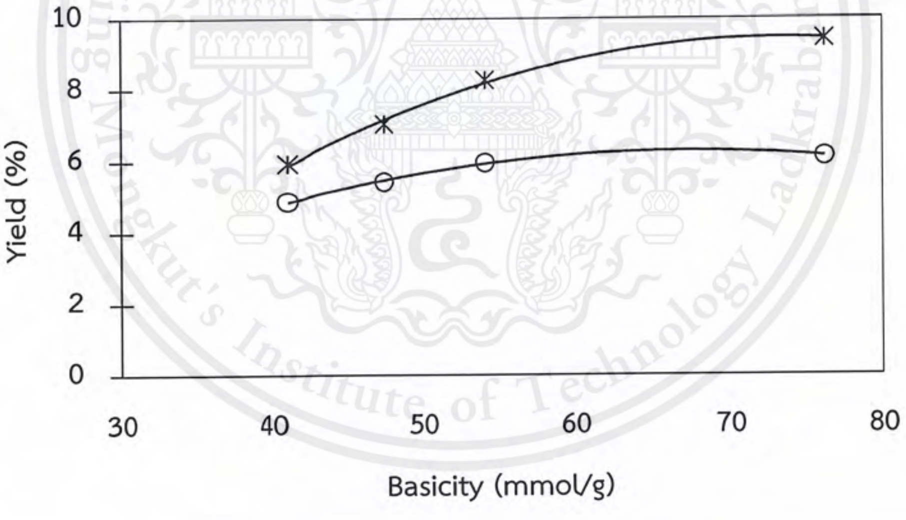

Figure 4.8 Effect of basicity on yield of products

✱ C4 alcohols, ○ Acetaldehyde

Higher activity of the cLDHs(3) is likely due to the appropriate strength of acid-base pairs, which improve the formation of acetaldehyde intermediate and coupling activity to higher alcohol molecules as shown in **Figure 4.7**. Accordingly, cLDHs(3) with Mg/Al ratio 3:1 is selected for further investigation.

4.2.2 Effect of contact time

In order to understand the reaction pathway for the product formation over the LDHs, effect of contact time on the ethanol conversion was investigated as presented in **Figure 4.9**

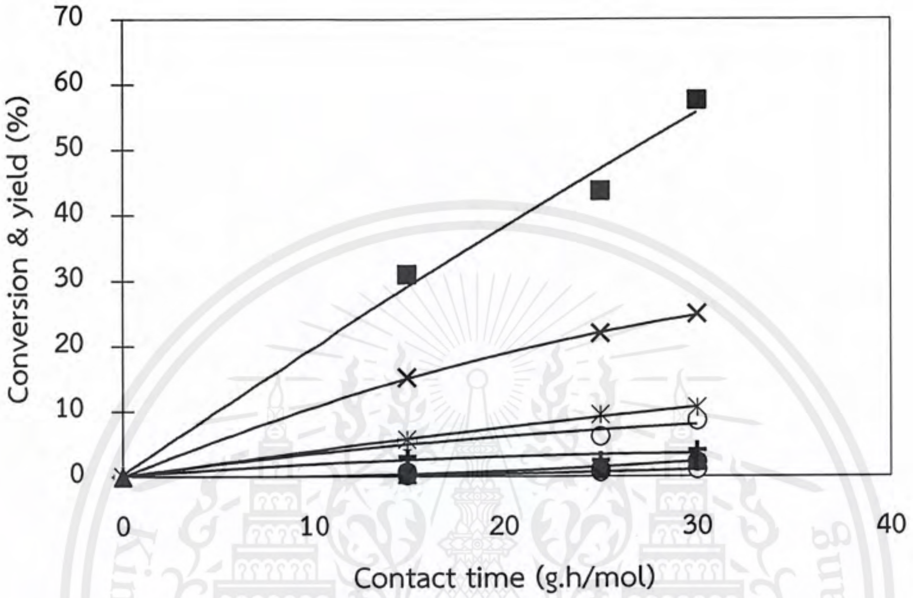

Figure 4.9 Conversion of ethanol and yields of products at various contact times *(Reaction condition; temperature: 380°C, pressure: 1 atm, contact time: 15-30 g.h/mol, flow rate of N_2 carrier gas: 60 mL/min, average result of time on stream)*
■ Conversion, × Ethylene, ✱ C4 alcohols, ○ Acetaldehyde, ⊠ Diethyl ether, ━ Acetone , △ Butanal, □ Diethyl acetal, ◆ C6 alcohols, ▲ C7 carbonyls

It is shown that the conversion of ethanol was doubled with doubling contact time (from 15 to 30 g.h/mol). This can be explained by increasing the amount of catalyst in the system which would consequently increase the numbers of active site for the reaction. The yield of ethylene was increased with contact time, due to dehydration of ethanol. However, no significant increase in yield of acetaldehyde was observed with increasing contact time. On the other hand, C4 alcohols yield was double as well as other higher alcohols and carbonyl products from further condensation of aldehyde as shown in **Table 4.3**.

Table 4.3 Conversion of ethanol and products yield over different contact time of cLDHs(3) catalyst.

Contact time (g.h/mol)	15	25	30
Conversion (%)	31.0	43.7	57.6
Yield of Product (%)			
Ethylene	15.1	21.9	24.8
Diethyl ether	3.1	2.5	4.0
Acetaldehyde	5.5	6.1	8.5
Acetone	0.2	0.7	1.1
Butanal	0.8	1.1	2.2
Diethyl acetal	0.2	-	0.5
Isobutylaldehyde dimethyl acetal	0.1	-	1.5
C4 alcohols(a)	5.7	9.4	10.5
C6 alcohols(b)	0.4	1.5	2.3
C7 alcohols(c)	-	-	0.4
C8 alcohols(d)	-	-	0.3
Aromatic alcohols(e)	-	-	-
C5 carbonyls(f)	-	-	0.5
C6 carbonyls(g)	-	-	0.5
C7 carbonyls(h)	-	0.4	0.8
C8 carbonyls(i)	-	-	0.4
C9 carbonyls(j)	-	-	-
Aromatic carbonyls(k)	-	-	-
Unknown	-	-	-

(a) : 1-Butanol and 2-Butenol

(b) : 2-Ethyl-1-butanol, 1-Hexanol and 3-Hexen-1-ol

(c) : 2,4-Dimethyl-2-pentanol

(d) : 2-Ethyl-1-hexanol and Octanol

(e) : Benzyl alcohol and 3,5-Diethylphenol

(f) : 2-Pentanone

(g) : Hexanal

(h) : 4-Heptanone and 3-Methylcyclohexanone

(i) : 2-Ethylhexanal and 2-Ethylcyclohexanone

(j) : 4-nonanone and 2-Ethylcyclohexanone

(k) : Benzaldehyde, 3-Methylbenzaldehyde, 4-Methylbenzaldehyde,
Acetophenone, 1-Phenyl-1-butanol and 4-Ethylacetophenone

(Reaction condition; temperature: 380°C, pressure: 1 atm, contact time: 25 g.h/mol, flow rate of N_2 carrier gas: 60 mL/min, average result from 6 h of time on stream)

According to Guerbet reaction, ethanol is primarily dehydrogenated to acetaldehyde (i). Then, the two acetaldehyde molecules undergo coupling via aldol condensation to crotonaldehyde (ii). The crotonaldehyde can be hydrogenated to butanal, an intermediate for butanol synthesis. Finally, butanal can be further hydrogenated to butanol (iii), as shown in **Scheme 4.1** and butanal can also be an intermediate for production of 2-ethyl-1-butanol (iv), as shown in **Scheme 4.2**. Some aldehydes may desorb and observed as carbonyl products while some could be hydrogenated to alcohol before desorption.

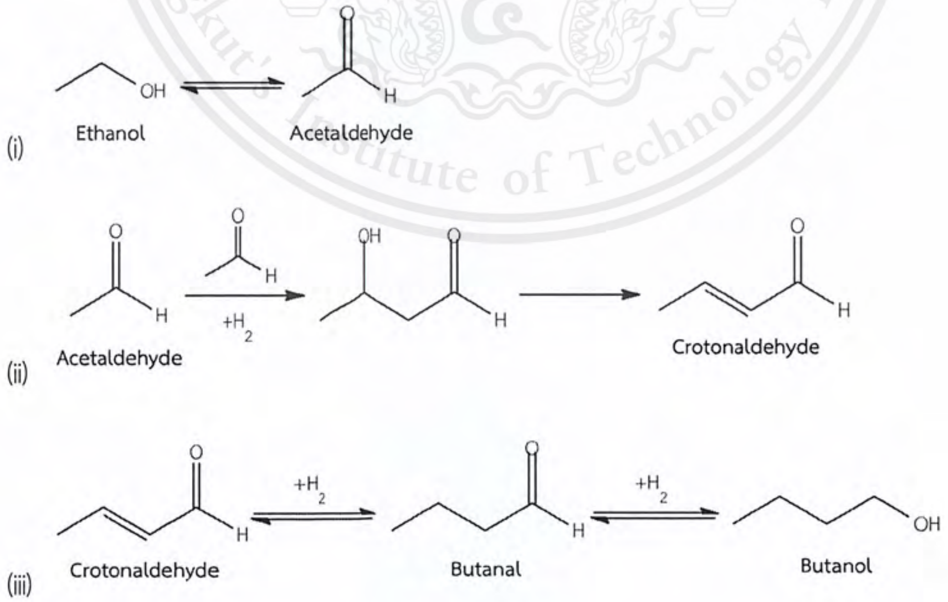

Scheme 4.1

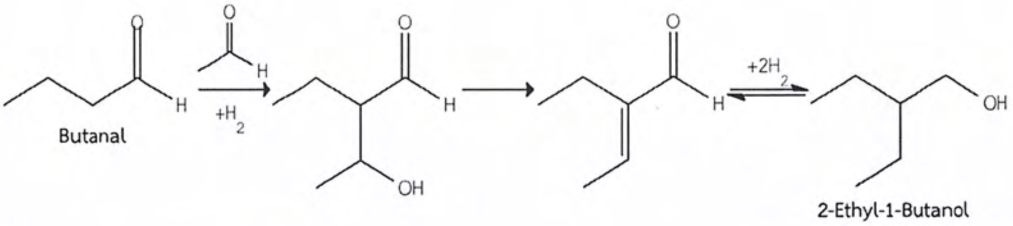

(iv)

Scheme 4.2

Moreover, acetone and C5-C7 carbonyls were also observed. These products may be resulted from decomposition of aldol intermediate to acetone and formaldehyde (v), which are served as condensing agents for the formation of C5-C7 carbonyls from C4-C6 aldehydes (vi), as shown in **Scheme 4.3**.

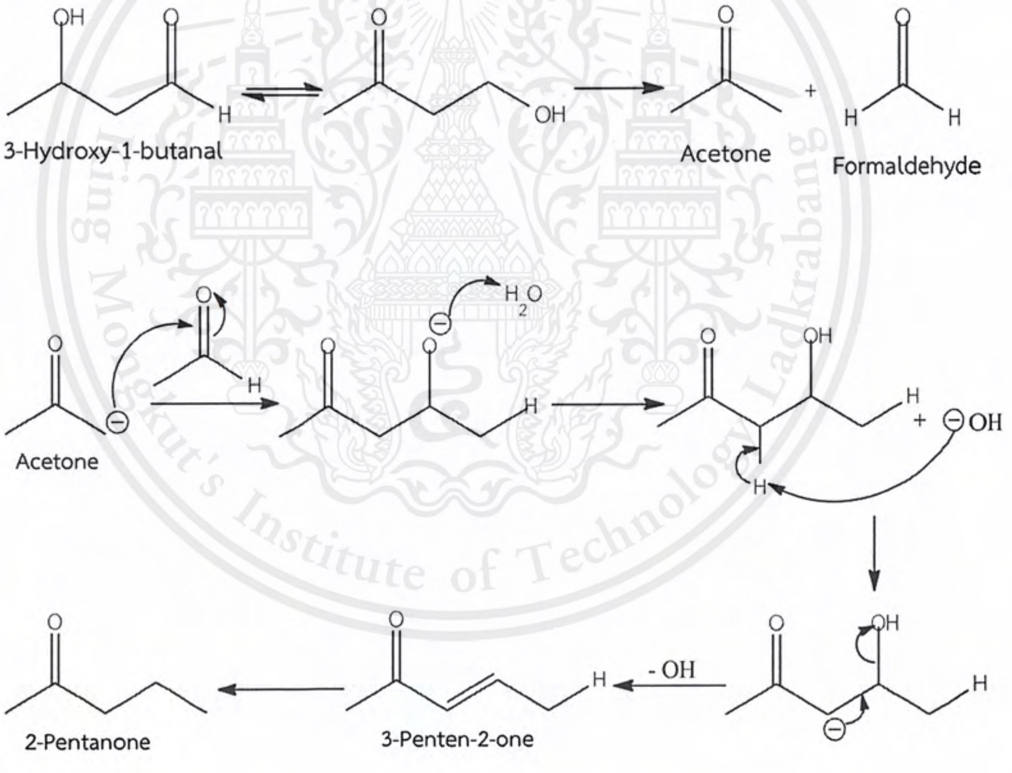

(v)

(vi)

Scheme 4.3

However, ethanol can also be converted in parallel to ethylene and diethyl ether. The ethylene formation can occur via monomolecular dehydration of ethanol over acid site (vii), while diethyl ether is formed via bimolecular dehydration of ethanol (viii), as seen in **Scheme 4.4**.

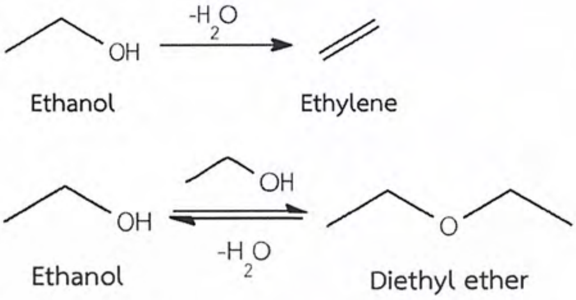

(vii)

(viii)

Scheme 4.4

It can be seen that all catalysts provide significant yield of undesired products, ethylene and diethyl ether. This is because cLDHs catalysts possess some acid sites that promote dehydration of ethanol. Hence, cLDHs should be modified with other metal oxide as investigated further.

4.2.3 Effect of metal incorporated cLDHs catalysts.

4.2.3.1 Influence of metal oxides co-precipitated cLDHs catalysts

In order to decrease acid sites and increase the active site for dehydrogenation, metal/Mg/Al mixed oxides (Cu-cLDHs, Zn-cLDHs, and Fe-cLDHs) were synthesized by substituting Mg^{2+} with Cu^{2+}, Zn^{2+} and Al^{3+} with Fe^{3+} in LDHs structure. The compositions of these catalysts are shown in **Table 4.1**. The activities for ethanol conversion of these catalysts are presented and compared with parents cLDHs(3) in **Table 4.4**.

Table 4.4 Ethanol conversion and yield of products over metal oxides co-precipitated cLDHs catalysts.

Catalysts	cLDHs(3)	Fe-cLDHs	Zn-cLDHs	Cu-cLDHs
Conversion (%)	43.7	45.0	50.1	40.78
Yield of Product (%)				
Ethylene	21.9	20.1	30.3	20.0
Diethyl ether	2.5	0.1	0.4	-
Acetaldehyde	6.1	12.7	6.7	9.5
Acetone	0.7	4.2	0.9	0.6
Butanal	1.1	0.8	1.3	1.6
Diethyl acetal	-	0.5	0.4	0.3
Isobutylaldehyde dimethyl acetal	-	1.3	0.1	-
C4 alcohols(a)	9.4	1.2	8.1	6.3
C6 alcohols(b)	1.5	-	1.1	0.5
C7 alcohols(c)	-	1.4	0.3	0.8
C8 alcohols(d)	-	0.3	-	0.2
Aromatic alcohols(e)	-	0.3	-	0.1
C5 carbonyls(f)	-	0.8	-	-
C6 carbonyls(g)	-	-	0.0	-
C7 carbonyls(h)	0.4	0.5	0.4	0.3
C8 carbonyls(i)	-	0.5	-	0.1
C9 carbonyls(j)	-	0.1	-	0.1
Aromatic carbonyls(k)	-	0.4	-	0.3
Unknown	-	-	-	-

(a) : 1-Butanol and 2-Butenol

(b) : 2-Ethyl-1-butanol, 1-Hexanol and 3-Hexen-1-ol

(c) : 2,4-Dimethyl-2-pentanol

(d) : 2-Ethyl-1-hexanol and Octanol

(e) : Benzyl alcohol and 3,5-Diethylphenol

(f) : 2-Pentanone

(g) : Hexanal

(h) : 4-Heptanone and 3-Methylcyclohexanone

(i) : 2-Ethylhexanal and 2-Ethylcyclohexanone

(j) : 4-nonanone and 2-Ethylcyclohexanone

(k) : Benzaldehyde, 3-Methylbenzaldehyde, 4-Methylbenzaldehyde, Acetophenone, 1-Phenyl-1-butanol and 4-Ethylacetophenone

(Reaction condition; temperature: 380°C, pressure: 1 atm, contact time: 25 g.h/mol, flow rate of N_2 carrier gas: 60 mL/min, average result from 6 h of time on stream)

Fe-cLDHs gives slightly higher conversion, as compared to cLDHs(3). It is clear that this catalyst provides high ethanol dehydrogenation activity as can be observed by the higher yield of acetaldehyde. However, Fe-cLDHs gives lower yield of higher alcohol, as compared to cLDH(3). This is consistent with the work done by M. Leon et al. [17]. They reported that the substitution of Al^{3+} by Fe^{3+} in the structure of LDHs leads to a slight decrease of the basic site. This would decrease rate of aldol condensation causing a lower yield of C4 alcohols. The substitution of Al^{3+} by Fe^{3+} was expected to help minimizing dehydration products. However, similar amount of undesired product ethylene, was obtained over Fe-cLDHs catalyst.

Zn-cLDHs shows a remarkably higher activity, as compared to other metal oxides and the parent cLDH. It can promote dehydrogenation of ethanol to acetaldehyde and also condensation of acetaldehydes to higher alcohols. However, the reaction over Zn-cLDHs gives high yield of undesired product, ethylene. In a different manner to Zn-cLDHs, Cu-cLDHs gives high yield of dehydrogenation product, acetaldehyde, but slight decrease in ethylene and diethyl ether yields. This is because Cu catalysts have redox properties together with good dispersion, that would promote dehydrogenation reaction. However, aldol condensation is suppressed. It can be seen that yield of higher alcohols are decreased because their basicities are decreased by replacing Mg^{2+} with Cu^{2+} and Zn^{2+}. Yield of ethylene from Zn-cLDHs is higher than that of Cu-cLDHs. NH_3-TPD insists that Zn-cLDHs has strong acidity site, as shown in **Figure 4.2(b)**, which promotes dehydration of ethanol.

According to the above results, Cu shows good activity in dehydrogenation of ethanol to acetaldehyde, an important intermediate for aldol condensation. However, these formed acetaldehydes are not readily condensed and hydrogenated to the higher alcohols over these metals modified cLDHs prepare by co-precipitation. This is probably due to low active surface for aldol condensation of the intermediate species.

4.2.3.2 Influence of metal and metal oxides impregnated cLDH by Cu-Zn alloy and adsorption Ru

With high dehydrogenation activity, together with low selectivity towards ethylene of Cu and high condensation activity of Zn, Cu-Zn alloy modified cLDHs catalysts were prepared by impregnation. Calcined (CuO-ZnO) and reduced Cu-Zn alloy (Cu-Zn) (at 400°C for 3 h) were investigated for ethanol conversion to higher alcohols. Ru oxide and Ru metal were also tested for Guerbet reaction as shown in **Table 4.5**.

Table 4.5 Ethanol conversion and yield of products over impregnation and adsorption cLDH catalysts.

Catalysts	cLDHs(3)	4Cu-0.8Zn /cLDHs	4Cu-0.8Zn /cLDHs (Re)	10Cu-2Zn /cLDHs	10Cu-2Zn /cLDHs (Re)	Ru /cLDHs	Ru /cLDHs (Re)
Conversion (%)	43.7	76.5	78.4	78.0	77.8	55.6	59.2
Yield of Product (%)							
Ethylene	21.9	12.2	14.6	9.8	15.9	19.3	23.5
Diethyl ether	2.5	1.2	0.7	1.9	1.6	1.4	1.0
Acetaldehyde	6.1	13.3	12.3	15.9	21.4	9.2	9.7
Acetone	0.7	0.7	1.1	0.7	1.3	1.0	1.3
Butanal	1.1	4.7	4.2	5.5	5.9	2.2	2.6
Diethyl acetal	-	1.0	0.8	0.9	1.2	0.5	0.8
Isobutylaldehyde dimethyl acetal	-	2.0	1.6	2.1	2.2	0.7	1.6
C4 alcohols(a)	9.4	8.5	8.2	7.8	6.3	10.4	9.2
C6 alcohols(b)	1.5	3.4	3.7	3.3	1.7	2.6	2.3
C7 alcohols(c)	-	2.3	1.9	2.1	3.7	0.7	0.8
C8 alcohols(d)	-	5.3	6.5	5.9	1.9	1.9	1.2
Aromatic alcohols(e)	-	0.9	1.0	1.1	1.3	0.2	0.1
C5 carbonyls(f)	-	2.0	1.5	2.0	1.8	0.6	0.9
C6 carbonyls(g)	-	1.2	1.2	1.4	1.0	0.5	0.5
C7 carbonyls(h)	0.4	2.0	2.2	1.9	1.3	1.0	1.1
C8 carbonyls(i)	-	3.1	3.5	3.4	1.5	0.7	1.0
C9 carbonyls(j)	-	2.0	2.0	1.8	0.8	0.4	0.4
Aromatic carbonyls(k)	-	9.9	10.6	9.6	6.6	2.2	1.3
Unknown	-	0.7	0.8	0.9	0.4	-	-

4Cu-0.8Zn/cLDHs : 4 wt.% Cu-0.8 wt.% Zn/cLDHs (impregnation)
10Cu-2Zn/cLDHs : 10 wt.% Cu-2 wt.% Zn/cLDHs (impregnation)

Ru/cLDHs : 1 wt.% Ru/cLDHs (adsorption)

*(Re) : Reduced at 400°C for 3 hours
(a) : 1-Butanol and 2-Butenol
(b) : 2-Ethyl-1-butanol, 1-Hexanol and 3-Hexen-1-ol
(c) : 2,4-Dimethyl-2-pentanol
(d) : 2-Ethyl-1-hexanol and Octanol
(e) : Benzyl alcohol and 3,5-Diethylphenol
(f) : 2-Pentanone
(g) : Hexanal
(h) : 4-Heptanone and 3-Methylcyclohexanone
(i) : 2-Ethylhexanal and 2-Ethylcyclohexanone
(j) : 4-nonanone and 2-Ethylcyclohexanone
(k) : Benzaldehyde, 3-Methylbenzaldehyde, 4-Methylbenzaldehyde, Acetophenone, 1-Phenyl-1-butanol and 4-Ethylacetophenone

(Reaction condition; temperature: 380°C, pressure: 1 atm, contact time: 25 g.h/mol, flow rate of N_2 *carrier gas: 60 mL/min, average result from 6 hours of time on stream)*

The conversions of ethanol over 4 wt.% Cu-0.8 wt.% Zn/cLDHs and 10 wt.% Cu-2 wt.% Zn/cLDHs were increased significantly, as compared to cLDHs(3). It is also seen that dehydration of ethanol to ethylene is significantly lower than cLDHs(3). This is because impregnation of Cu and Zn on cLDHs(3) surface may suppress the strong acid site as shown by a shift to lower temperature of NH_3-TPD, especially for 4 wt.% Cu-0.8 wt.% Zn/cLDH (**Figure 4.2(c)**).

In turn, yield of acetaldehyde is increased because dehydrogenation of ethanol is promoted as well as condensation of acetaldehyde to higher alcohols and carbonyl compounds. It is clear that Cu-Zn impregnated cLDHs has good activity in dehydrogenation of ethanol to acetaldehyde but not readily active for hydrogenation of the carbonyl compounds to alcohols. Reduced and non-reduced 4 wt.% Cu-0.8 wt.% Zn/cLDHs have similar activity. One of the reasons could be that Cu might have already been reduced with Zn during calcination. This is because no reduction peak was observed in TPR of 4 wt.% Cu-0.8 wt.% Zn alloy/cLDHs (**Figure 4.6**).

Increase in loading of the metal from 4.8 wt. % to 12 wt.% consequently lower the yield of ethylene and alcohols. However, 10 wt.% Cu-2 wt.% Zn/cLDHs gives lower yield of acetaldehyde, as compared to 4 wt.% Cu-0.8 wt.% Zn/cLDHs. This may be the effect of the Cu-Zn alloy obscures acid and basic sites, which suppresses both dehydration and aldol condensation.

However, at similar conversions, non-reduced 10 wt.% Cu-2 wt.% Zn/cLDHs gives higher yield of higher alcohols, as compared to the reduced sample. This is because Cu and Zn oxides is retained in the reduced sample, as evidenced by TPR (**Figure 4.6(c)**). This species can promote dehydrogenation of ethanol and also condensation of acetaldehyde to higher alcohols. The reduced sample also give higher yield of ethylene, presumably due to the existence of acid site forming after reduction at 170°C (**Figure 4.6**).

In order to increase the active site for hydrogenation of higher carbonyl compounds, the Ru adsorbed cLDHs was tested for the conversion of ethanol as shown in **Table 4.3**. This is because Ru is one of the metals used extensively as a catalyst for hydrogen transfer [44].

As compared to cLDHs(3), 1 wt.% Ru/cLDHs gives higher conversion and yield of higher alcohols. It clear that the Ru sample provides high ethanol dehydrogenation activity as can be seen by the higher yield of acetaldehyde. Higher alcohols (C4 alcohols) are especially increased and small amounts of carbonyl products can be observed. It show that Ru has better aldol condensation and hydrogenation activity, as compared to that of cLDHs(3). However, yield of ethylene is remain high (~19-23%) over 1 wt.% Ru/cLDHs.

The reduced 1 wt.% Ru/cLDHs shows higher activity, as compared to the non-reduced catalysts. However, this catalyst also provides dehydration activity as seen by the higher yield of ethylene. Since metallic Ru decrease basicity site and dehydrogenation activity, increase selectivity for dehydration of ethanol was observed. The non-reduced 1wt%Ru/cLDHs gives slightly higher yield of higher alcohols because ruthenium oxides would higher possess basicity site (**Table 4.5**). Moreover, lower yield of higher carbonyl compounds were observed over 1 wt.% Ru/cLDHs, as compared to Cu-Zn alloy/cLDHs prepared by impregnation.

CHAPTER 5

CONCLUSIONS AND SUGGESTIONS

5.1 Conclusions

Calcined LDHs with Mg/Al ratio 3:1 (cLDHs(3)) show higher activity for higher alcohols production from ethanol, as compared to the other cLDHs (Mg/Al molar ratios 1:1, 2:1 and 6:1). Correlations between selectivity of products and acidic-basic properties were observed. It is important to tune and balance the number and strength of acid and basic sites, in order to obtain high selectivity of desired products in the Guerbet reaction.

XRD shows that before calcination, LDHs are lamella materials. After calcination at 450°C, the layered structure of LDHs was completely collapsed due to removal of carbonate and hydroxyl groups. TPD data shows that basic sites are decreased when cLDHs was incorporated with metal oxides i.e. Cu, Zn and Fe, presumably because the basic sites are obscured by the incorporated metal oxides.

Higher alcohols occur via Guerbet reaction and ethylene production occurs by dehydration, as parallel reaction. The yield of higher alcohols increased with contact time. Acetaldehyde was increased with basicity.

Fe-cLDHs give lower yield of higher alcohol, as compared to the parent cLDHs(3), because replacing Al^{3+} with Fe^{3+} leads to a decrease in the basic site. This would decrease rate of aldol condensation causing a lower yield of C4 alcohols, but offer similar amount of undesired ethylene product. Zn-cLDHs and Cu-cLDHs show a higher activity, as compared to Fe-cLDHs and the cLDH(3). It can promote formation of acetaldehyde, an important intermediate for aldol condensation to larger molecules. On the other hand, aldol condensation is suppressed by replacing Mg^{2+} with Cu^{2+} and Zn^{2+} because their basicity is decreased.

The Cu-Zn impregnated cLDHs (Cu-Zn/cLDHs) also show higher activity for dehydrogenation of ethanol and aldol condensation of acetaldehyde, as compared to cLDHs(3). The Cu-Zn/cLDHs is not readily active for hydrogenation of the higher carbonyl compounds to produce higher alcohols. Moreover, dehydration of ethanol to ethylene is suppressed over Cu-Zn/cLDHs. The yields of butanol over reduced and non-reduced 4 wt.% Cu-0.8 wt.% Zn/cLDHs are similar because Cu had already been reduced with Zn during calcination. However, non-reduced 10 wt.% Cu-2 wt.% Zn/cLDHs give higher yield of higher alcohols, as compared to the reduced one. This is because non-reduced Cu-Zn mixed oxides promote dehydrogenation of ethanol. Reduced 10 wt.% Cu-2 wt.% Zn/cLDHs show the existence of acid sites, which affect dehydration of ethanol to ethylene. Nevertheless, increasing the loading of the metal from 4.8 wt.% to 12 wt.% consequently lowers the yield of both ethylene and higher alcohols. This may be the effect of the alloy obscures acid and basic sites, which suppresses both dehydration and aldol condensation.

The Ru adsorbed cLDHs promotes aldol condensation and hydrogenation of carbonyl compounds for production of higher alcohols (C4 alcohols). Reduced 1 wt.% Ru/cLDHs shows higher activity, as compared to non-reduced catalysts. However, the reduced catalyst provides more undesired ethylene. The non-reduced 1 wt.% Ru/cLDHs gives slightly higher yield of higher alcohols, as compared to the reduced sample because Ru oxides would possess higher basicity, as compared to that of Ru metal.

5.2 Suggestions for future studies

5.2.1 The effect of Ru oxides loadings over cLDHs on ethanol conversion activity should be further studied.

5.2.2 The effect of Cu-Zn oxides loadings over cLDHs on ethanol conversion activity should be further investigated.

5.2.3 The ethanol conversion activity of Cu-Ru oxides/cLDHs should be further attended.

REFERENCES

[1] Marcu, I. Tanchoux, N. Fajula, F. Tichi, D. 2013. "Catalytic Conversion of Ethanol into Butanol over M–Mg–Al Mixed Oxide Catalysts (M 5 Pd, Ag, Mn, Fe, Cu, Sm, Yb) Obtained from LDH Precursors." *Catal Lett.* 143 : 23-30.

[2] Joseph, T. Kozlowski, R. Davis, J. 2013. "Heterogeneous Catalysts for the Guerbet Coupling of Alcohols." *ACS Catal.* 3 : 1588-1600.

[3] **Layer double hydroxides.** [Online].
Available : https://en.wikipedia.org/wiki/Layered_double_hydroxides.

[4] **Alcohols.** [Online]. Available : http://goldbook.iupac.org/A00204.html.

[5] Gerhartz, W. Stephen, Y. Yamamoto, Thomas, F. Pfefferkorn, F. And Rounsaville, F. 1999. "Abrasives to Aluminum Oxide." *Ullmmann's Encyclopedia of Industrial Chemistry.* vol. A1 : 279-282.

[6] **Reactions of Alcohols.** [Online]. Available : http://2012books.lardbucket.org.

[7] **Ethanol**. [Online]. Available : http://http://en.wikipedia.org.

[8] Prof. Shakhashiri. **Chemical of the week, Ethanol.** [Online].
Available : www.scifun.org

[9] Gerhartz, W. Stephen, Y. Yamamoto, Thomas, F. Pfefferkorn, F. and Rounsaville, F. 1999 "Dithiocarbamic Acid to Ethanol.Ullmmann's." *Encyclopedia of Industrial Chemistry.* vol. A9 : 588-590.

[10] **Butanol.** [Online]. Available : https://en.wikipedia.org.

[11] **n-Butanol.** [Online]. Available :
http://www.centralmnrenewables.com/images/E0068001/WhatisButanol.pdf

[12] **1-Hexanol.** [Online].
Available : https://en.wikipedia.org/wiki/1Hexanol#Occurrence_in_Nature

[13] **1-Octanol.** [Online]. Available : https://en.wikipedia.org

[14] **Benzyl Alcohol.** [Online]. Available : http://www.chemicalland21.com

[15] **Aldehyde.** [Online].
Available : https://global.britannica.com/science/Aldehyde

[16] **Aetaldehyde.** [Online]. Available : https://en.wikipedia.org/wiki/Acetaldehyde

[17] **Butyraldehyde.** [Online].

Available : https://en.wikipedia.org/wiki/Butyraldehyde

[18] **Hexanal.** [Online]. Available : https://en.wikipedia.org/wiki/Hexanal

[19] Haynes, W.M. 2014 CRC Handbook of Chemistry and Physics. 95th ed. CRC press. 3-34.

[20] Andersen, A. 2006. “Final report on the safety assessment of benzaldehyde.” *International Journal of Toxicology.* 25(1) : 11–27.

[21] Leon, M. Diaz, E. Vega, A. Ordonez, S. and Auroux, A. 2011. “Consequences of the iron-aluminium exchange on the performance of hydrotalcite derived mixed oxide for ethanol condensation.” *Applied Catalysis B: Environmental.* 102 : 590-599.

[22] Earley, J. H. Bourne, R. A. Watson, M. J. and Poliakoff, M. 2015. “Continuous catalytic upgrading of ethanol to n-butanol and >C4 products over Cu/CeO2 catalysts in supercritical CO2.” *Green Chemistry.* 17 : 3018-3025.

[23] Di Cosimo, J.I. Apesteguia, C.R. Ginés M.J.L. and Iglesia, E. 2000. “Structural Requirements and Reaction Pathways in Condensation Reaction of Alcohol on Mg_yAlO_xCatalysts.” *Journal Catalysis.* 190 : 261-275.

[24] **Catalyst.** [Online].

Available : http://www.chemicool.com/definition/catalyst.html

[25] Pang, J. Zheng, M. He, L. Li, L. Pan, X. Wang, A. Wang, X. and Zhang, T. 2016. “Upgrading ethanol to n-butanol over highly dispersed Ni-MgAlO catalysts.” *Journal of Catalysis.* 344 : 184-193.

[26] Frederick, L. Godwin, A. and Ray L. 2016 “Synthesis of layered double Hydroxides containing $Mg^{2+,}$ Zn^{2+}, $Ca^{2+}$and Al^{3+} layer cations by co-precipitation methods-A review.” *Applied Surface Science.* 383 : 200-213.

[27] Juan, J. Edgar, A. and Oyama, S. T. 2004. "Review of the synthesis of LayeredDouble Hydroxides: Thermodynamic Apporach." *Quim. Nova*. 27 : 601-614.

[28] Luíz, P. Rejane, A. Júnia, A. Denise, E. Rodrigo, M. Leonardo, A.Leonardus, V. Roberto, F. Liovando, M. Frederico, G. and Jairo, T. 2015. "Layered Double Hydroxides: Nanomaterial for Application in Agriculture." *Revisao de Literatura.* 39 : 1-13.

[29] Scalbert, J. Thibault-Starzyk, F. Jacquot, R. Morvan, D. and Meunier, F. 2014. "Ethanol condensation to butanol at higher temperatures over a basic heterogeneous catalyst: How relevant is acetaldehyde self-aldolization?" *Journal of Catalysis*. 311 : 28-32.

[30] Seftel, E.M. Popovici, E. Mertens, M. De Witte, K. Van Tendeloo, G. Cool, P. and Vansant, E.F. 2008. "Zn-Al layered double hydroxides: Synthesis, characterization and photocatalytic application." *Microporous and Mesoporous Materials*. 113 : 296-304.

[31] Dudek, B. Kustrowski, P. Bialas, A. Natkanski, P. Piwowarska, Z. Chmielarz, L.Kozak, M. and Michalik, M. 2012. "Infiuence of textural and structural properties of Mg-Al and Mg-Zn-Al containing hydrotalcite derived oxides on Cr(VI) adsorption capacity." *Materials Chemistry and Physics*. 132 : 929-936.

[32] Zeng, Y. Zhang, T. YueyangXu, Ye, T. Wang, R. Yang, Z. Jia, Z. and Ju, Z. 2016. "Cu/Mg/Al hydrotalcite-like hydroxide catalysts for o-phenylphenol synthesis." *Applied Clay Science*. 126 : 207-214.

[33] Marcu, I. Tichit, D. Fajula, F. and Tanchoux. N. 2009. "Catalytic valorization of bioethanol over Cu-Mg-Al mixed oxide catalysts." *Catalysis Today.* : 231- 238.

[34] Shiau, C.Y. Chen, S, Tsai, J.C. and Lin, S.I. 2000. "Effect of zinc addition on copper catalyst in isoamyl alcohol dehydrogenation" *Applied Catalysis: Gerneral*. 198 : 95-102

[35] Li, D. Li, R. Lu, M. Lin, X. Zhan, Y. and Jiang, L. 2017. “Carbon dioxide reforming of methane over Ru catalysts supported on Mg-Al oxides: A highly dispersed and stable Ru/Mg(Al)O catalyst.” *Applied Catalysis B: Environmental.* 200 : 566–577.

[36] Lee, S.H. and Moon, D.J. 2011. “Studies on the conversion of glycerol to 1,2-propanediol over Ru-based catalyst under mild conditions.” *Catalysis Today.* 174 : 10– 16

[37] Climent, M.J. Corma, A. Iborra, S. Epping, K. and Velty, A. 2004. “Increasing the basicity and catalytic activity of hydrotalcites by different synthesis procedures.” *Journal of Catalysis.* 225 : 316-326.

[38] Teixeira, T.P.F. Aquin, S.F. Pereira, S.I. and Dias, A. 2014. “Use of calcined layered double hydroxides for the removal of color and organic matterfrom textile effluents: kinetic, equilibrium and recycling studies.” *Brazilian Journal of Chemical Engineering.* 31(1) : 19-26.

[39] Wang, Q. Wu, Z. Tay, H. Chen, L. Yiu, Y. Chang, J. Zhong, Z. Luo, J. and Borgna, A. 2011. “High temperature adsorption of CO_2 on Mg–Al hydrotalcite: Effect of the charge compensating anions and the synthesis pH.” *Catalyst Today.* 164 : 198-203.

[40] M. Mohan Rao, B. Ramachandra Reddy, M. Jaylakshmi, V. Swarna Jaya, B. Sridhar . 2005. “Hydrothermal synthesis of Mg-Al hydrotalcites by urea hydrolysis.” *Materials Research Bulletin.* 40 : 347-359.

[41] Manriquez, M.E. Hernandez-Cortez, J.G. Wang, J.A. Chen, L.F. Zuniga Moreno, A. and Gomez, R. 2015. “Synthesis of transition metal doped lamellar double hydroxides as base catalysts for acetone aldol condensation.” *Applied Clay Science.* 118 : 188-194.

[42] Zhijian, L. 2005. “Novel solid base catalysts for Michael additions Synthesis, Characterization and Application.” M.Sc Thesis of Humboldt University of Berlin.

[43] MeiraI, D.M. CortezI, G.G. MonteiroII, W.R. and RodriguesII, J.A.J. 2006. "Vanadium oxides supported on hydrotalcite-type precursors: the effect of acid-base properties on the oxidation of isopropanol." *Brazilian Journal of Chemical Engineering.* 23(3) : 351-358.

[44] Hamid, S.A. Slatford, A. and Williams, M.J. 2007. "Borrwing Hydrogen in the Activation of Alcohols." *Advanced Synthesis and Catalysis*. 349(10) : 1555-1575.

APPENDICES

APPENDIX A

CALCULATION

Contact time, W/F

Calculation of catalytic parameter

$$W/F = \frac{\text{Weight of catalyst (g)}}{\text{Molar feed rate (mol/h)}}$$

In the reaction using 0.7 mol/h of ethanol in feed and using 0.3 grams of catalyst, the W/F is calculated as follow:

$$W/F = \frac{[\ 0.3 \text{ g cat.}\ ]\ [\ 46 \text{ gEtOH/mol}\ ]}{[\ 0.7 \text{ mL/h}\ ]\ [\ 0.789 \text{ gEtOH/mL}\ ]}$$

$$= 25 \text{ g.h/mol}$$

In similar manner; W/F of catalysts with different catalyst weight and different feed rate are calculated.

Calculation of % yield of products from gas chromatography

Table A1 The summation of the peak area of products.

Product	Peak area
Ethylene	1422321
Diethyl ether	161618
Acetaldehyde	1347146
Acetone	79070
Butanal	422546
Diethyl acetal	68704
Isobutylaldehyde dimethyl acetal	103073
C4 alcohol	758916
C6 alcohol	316008
C7 alcohol	173500
C8 alcohol	574619
Aromatic alcohol	34119
C5 carbonyl	104307
C6 carbonyl	74050
C7 carbonyl	209456
C8 carbonyl	284099
C9 carbonyl	177815
Aromatic carbonyl	1053116
Unknown	56966
Ethanol (Feed)	2080348
Total	9501797

*Information of 4 wt.% Cu-0.8 wt.% Zn/cLDHs in ethanol, contact time =25 g.h/mol, time on stream = 60 minutes, flow rate of carrier gas: N_2 at 60 mL/min

In normalization method, the areas of all eluted peak were computed areas for differences in the detector response to different compound types. The concentration of the analyzed was found from the ratio of its area to the total area of all peaks.

Calculate the percent yield of each component in sample as follows:

$$\%\text{Yield in each product} = \frac{\text{Peak area of A} \times 100}{\text{Total area}}$$

Where A is each product.

For example;

$$\%\text{Yield of Ethylene} = \frac{1422321 \times 100}{9501797}$$

$$= 14.969$$

The percent yield of each product obtained from above calculation is shown in **Table A2**.

Table A2 Yield of product derived by normalization method.

Product	Yield (%)
Ethylene	14.969
Diethyl ether	1.701
Acetaldehyde	14.178
Acetone	0.832
Butanal	4.447
Diethyl acetal	0.723
Isobutylaldehyde dimethyl acetal	1.085
C4 alcohol	7.987
C6 alcohol	3.326
C7 alcohol	1.826
C8 alcohol	6.047
Aromatic alcohol	0.359
C5 carbonyl	1.098
C6 carbonyl	0.779
C7 carbonyl	2.204
C8 carbonyl	2.990
C9 carbonyl	1.871
Aromatic carbonyl	11.083
Unknown	0.600
Ethanol (Feed)	21.894
Total	100

Conversion

%Conversion can be calculated from the following equation:

$$\%\text{Conversion} = \frac{(\text{Area total} - \text{Area feed}) \times 100}{\text{Area total}}$$

For example;

$$\%\text{Conversion} = \frac{(9501797-2080348) \times 100}{9501797}$$

$$= 78.11$$

Selectivity

%Selectivity can be obtained from the following equation:

$$\%\text{Selectivity in each product} = \frac{\%\text{Yield of each product} \times 100}{\%\ \text{Conversion}}$$

For example;

$$\%\text{Selectivity of Ethylene} = \frac{14.969 \times 100}{78.11}$$

$$= 19.16$$

APPENDIX B

GAS CHROMATOGRAM

Analysis of gas product from gas chromatography

Prior to analysis, the structure of each products in the sample is identified the by GC-MS (gas chromatography with mass spectrometer detector). Then, the quantitative analysis of each product was carried out by GC-FID (gas chromatography with flam ionization detector) with the condition expressed in **Table B1**.

Table B1 The GC condition for quantitative analysis

Column	FFAP, 30 m x 0.32 mm x 0.25 µm
Temperature program	35°C (2 min hold) to 200°C at 15°C/min
Carrier gas	Nitrogen at 60 mL/min
Injection	250°C
Detector	FID

The chromatogram of gas products were identified using reference standard for comparison in **Table B2**

Table B2 Chromatogram data of standard product distribution and feed

Feed and Products	Retention time (min)
Ethylene	1.912
Diethyl ether	2.036
Acetaldehyde	2.180
Acetone	2.604
Butanal	2.960
Diethyl acetal	3.149
Ethanol	3.434
Isobutylaldehyde dimethyl acetal	3.862
2-Pentanone	4.065

2,4-Dimethyl-2-pentanol	4.634
Hexanal	4.994
4-Heptanone	5.459
1-Butanol	5.800
2-Ethylhexanal	6.201
2-Buten-1-ol, (E)-	6.641
2-Buten-1-ol	7.041
2-Ethyl-1-butanol	7.502
3-Methylcyclohexanone	7.790
4-Nonanone	7.899
1-Hexanol	7.985
3-Hexen-1-ol, (E)-	8.097
2-Ethylcyclohexanone	8.421
2-Ethylcycloheptanone	8.739
2-Ethyl-1-hexanol	9.307
Benzaldehyde	9.907
Octanol	10.090
3-Methylbenzaldehyde	10.778
4-Methylbenzaldehyde	10.778
Acetophenone	11.060
1-Phenyl-1-butanone	11.935
4-Ethylacetophenone	12.231
Benzyl alcohol	12.443
3,5-Diethylphenol	12.823

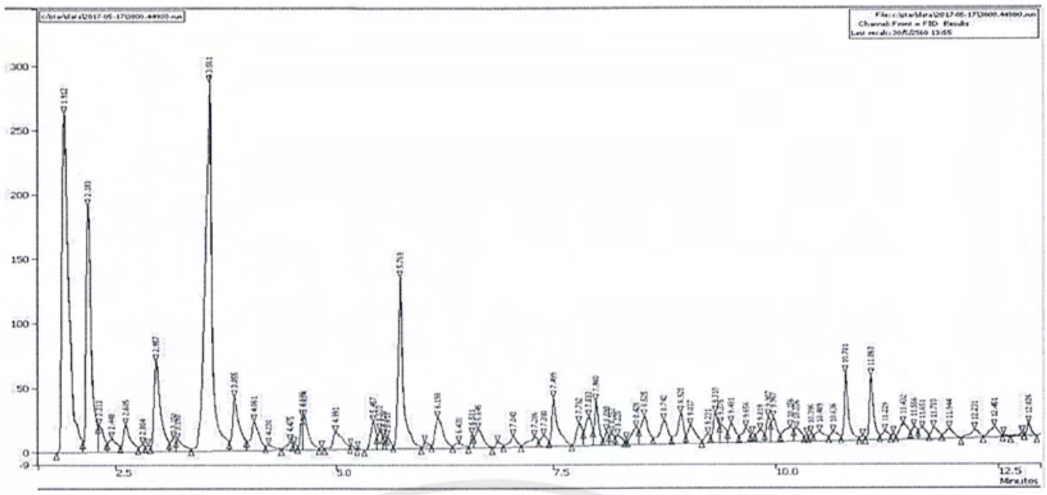

Figure B1 Chromatogram of products over 4 wt.% Cu-0.8 wt.% Zn/cLDH at W/F = 25 g.h/mol at 380°C

APPENDIX C

REACTION DATA

1. Conversion of ethanol to higher alcohols over various cLDHs

1.1 Ethanol conversion over cLDHs(1)

Table C1 The ethanol conversion and yield of products of cLDHs(1)

Time on stream (min)	60	120	180	240	300	360
Conversion (%)	39.0	42.6	42.1	34.2	37.1	41.1
Yield of product (%)						
Ethylene	26.4	29.1	28.9	22.5	24.5	28.0
Diethyl ether	0.6	0.6	0.6	0.8	0.5	0.6
Acetaldehyde	4.6	4.9	4.9	4.4	4.4	4.8
Acetone	0.7	0.8	1.1	0.8	0.9	1.1
Butanal	0.7	0.7	0.7	0.5	0.6	0.7
Diethyl acetal	0.0	0.0	0.0	0.0	0.0	0.0
Isobutylaldehyde dimethyl acetal	0.0	0.0	0.0	0.0	0.0	0.0
C4 alcohols	5.2	5.5	4.9	4.5	5.3	5.0
C6 alcohols	0.4	0.5	0.5	0.4	0.4	0.5
C7 alcohols	0.0	0.0	0.0	0.0	0.0	0.0
C8 alcohols	0.0	0.0	0.0	0.0	0.0	0.0
Aromatic alcohols	0.0	0.0	0.0	0.0	0.0	0.0
C5 carbonyls	0.0	0.0	0.0	0.0	0.0	0.0
C6 carbonyls	0.0	0.0	0.0	0.0	0.0	0.0
C7 carbonyls	0.4	0.5	0.5	0.3	0.4	0.5
C8 carbonyls	0.0	0.0	0.0	0.0	0.0	0.0
C9 carbonyls	0.0	0.0	0.0	0.0	0.0	0.0
Aromatic carbonyls	0.0	0.0	0.0	0.0	0.0	0.0
Unknown	0.0	0.0	0.0	0.0	0.0	0.0

(Reaction condition; temperature: 380°C, pressure: 1 atm, contact time: 25 g.h/mol, flow rate of N_2 carrier gas: 60 mL/min)

1.2 Ethanol conversion over cLDHs(2)

Table C2 The ethanol conversion and yield of products of cLDHs(2)

Time on stream (min)	**60**	**120**	**180**	**240**	**300**	**360**
Conversion (%)	53.1	47.6	52.0	48.5	52.2	45.8
Yield of product (%)						
Ethylene	34.9	29.3	32.7	30.4	33.7	28.6
Diethyl ether	0.6	0.9	0.8	0.8	0.7	0.9
Acetaldehyde	6.0	5.7	6.0	6.0	6.0	5.7
Acetone	0.7	0.6	0.7	0.4	0.7	0.4
Butanal	1.0	0.9	1.0	0.9	1.0	0.9
Diethyl acetal	0.0	0.3	0.3	0.3	0.3	0.3
Isobutylaldehyde dimethyl acetal	0.0	0.0	0.0	0.0	0.0	0.0
C4 alcohols	8.2	8.2	8.7	8.2	8.2	8.1
C6 alcohols	1.3	1.0	1.3	1.1	1.1	0.8
C7 alcohols	0.0	0.0	0.0	0.0	0.0	0.0
C8 alcohols	0.0	0.0	0.0	0.0	0.0	0.0
Aromatic alcohols	0.0	0.0	0.0	0.0	0.0	0.0
C5 carbonyls	0.0	0.0	0.0	0.0	0.0	0.0
C6 carbonyls	0.0	0.0	0.0	0.0	0.0	0.0
C7 carbonyls	0.4	0.3	0.4	0.3	0.4	0.3
C8 carbonyls	0.0	0.0	0.0	0.0	0.0	0.0
C9 carbonyls	0.0	0.0	0.0	0.0	0.0	0.0
Aromatic carbonyls	0.0	0.3	0.0	0.0	0.0	0.0
Unknown	0.0	0.0	0.0	0.0	0.0	0.0

(Reaction condition; temperature: 380°C, pressure: 1 atm, contact time: 25 g.h/mol, flow rate of N_2 carrier gas: 60 mL/min)

1.3 Ethanol conversion over cLDHs(3)

Table C3 The ethanol conversion and yield of products of cLDHs(3)

Time on stream (min)	**60**	**120**	**180**	**240**
Conversion (%)	45.1	45.9	40.7	49.1
Yield of product (%)				
Ethylene	22.0	23.0	19.9	28.8
Diethyl ether	2.7	2.7	2.7	1.0
Acetaldehyde	6.3	6.3	5.9	6.3
Acetone	0.7	0.7	0.6	0.8
Butanal	1.2	1.2	1.0	1.1
Diethyl acetal	0.0	0.3	0.0	0.0
Isobutylaldehyde dimethyl acetal	0.0	0.0	0.0	0.0
C4 alcohols	10.0	9.6	8.9	9.1
C6 alcohols	1.7	1.6	1.3	1.5
C7 alcohols	0.0	0.0	0.0	0.0
C8 alcohols	0.0	0.0	0.0	0.0
Aromatic alcohols	0.0	0.0	0.0	0.0
C5 carbonyls	0.0	0.0	0.0	0.0
C6 carbonyls	0.0	0.0	0.0	0.0
C7 carbonyls	0.5	0.5	0.4	0.5
C8 carbonyls	0.0	0.0	0.0	0.0
C9 carbonyls	0.0	0.0	0.0	0.0
Aromatic carbonyls	0.0	0.0	0.0	0.0
Unknown	0.0	0.0	0.0	0.0

(Reaction condition; temperature: 380°C, pressure: 1 atm, contact time: 25 g.h/mol, flow rate of N_2 *carrier gas: 60 mL/min)*

1.4 Ethanol conversion over cLDHs(6)

Table C4 The ethanol conversion and yield of products of cLDHs(6)

Time on stream (min)	**60**	**120**	**180**	**240**	**300**	**360**
Conversion (%)	53.3	46.2	49.8	50.5	56.4	45.4
Yield of product (%)						
Ethylene	31.6	26.0	29.4	30.7	39.0	27.1
Diethyl ether	4.5	4.9	4.6	4.4	1.1	4.4
Acetaldehyde	5.4	5.3	5.5	5.5	5.6	5.2
Acetone	0.6	0.6	0.7	0.7	0.9	0.6
Butanal	0.8	0.8	0.9	0.9	1.0	0.8
Diethyl acetal	0.0	0.2	0.2	0.2	0.2	0.2
Isobutylaldehyde dimethyl acetal	0.0	0.0	0.0	0.0	0.0	0.0
C4 alcohols	8.0	7.3	7.3	7.2	7.3	6.6
C6 alcohols	1.3	0.8	0.8	0.9	1.0	0.5
C7 alcohols	0.0	0.0	0.0	0.0	0.0	0.0
C8 alcohols	0.0	0.0	0.0	0.0	0.0	0.0
Aromatic alcohols	0.2	0.0	0.2	0.0	0.0	0.0
C5 carbonyls	0.0	0.0	0.0	0.0	0.0	0.0
C6 carbonyls	0.0	0.0	0.0	0.0	0.0	0.0
C7 carbonyls	0.3	0.3	0.3	0.0	0.2	0.0
C8 carbonyls	0.0	0.0	0.0	0.0	0.0	0.0
C9 carbonyls	0.0	0.0	0.0	0.0	0.0	0.0
Aromatic carbonyls	0.4	0.0	0.0	0.0	0.0	0.0
Unknown	0.0	0.0	0.0	0.0	0.0	0.0

(Reaction condition; temperature: 380°C, pressure: 1 atm, contact time: 25 g.h/mol, flow rate of N_2 carrier gas: 60 mL/min)

1.5 Ethanol conversion over Fe-cLDHs catalyst

Table C5 The ethanol conversion and yield of products over Fe-cLDHs catalyst

Time on stream (min)	**60**	**120**	**240**	**300**	**360**
Conversion (%)	42.7	44.9	44.0	44.0	42.4
Yield of product (%)					
Ethylene	20.8	21.4	20.2	17.0	16.4
Diethyl ether	0.2	0.0	0.0	0.0	0.0
Acetaldehyde	12.4	14.0	14.0	11.8	11.8
Acetone	3.8	4.2	4.3	3.5	3.4
Butanal	0.7	0.8	0.9	0.8	0.8
Diethyl acetal	0.5	0.5	0.4	0.4	0.4
Isobutylaldehyde dimethyl acetal	0.5	0.8	0.6	2.2	2.2
C4 alcohols	1.1	0.9	0.8	1.4	1.4
C6 alcohols	0.0	0.0	0.0	0.0	0.0
C7 alcohols	1.3	1.3	1.5	1.2	1.3
C8 alcohols	0.0	0.0	0.0	0.7	0.7
Aromatic alcohols	0.0	0.0	0.0	1.2	0.7
C5 carbonyls	0.9	0.8	0.8	0.6	0.6
C6 carbonyls	0.0	0.0	0.0	0.0	0.0
C7 carbonyls	0.0	0.0	0.0	1.3	1.2
C8 carbonyls	0.4	0.5	0.5	0.4	0.4
C9 carbonyls	0.0	0.0	0.0	0.3	0.3
Aromatic carbonyls	0.0	0.0	0.0	1.0	0.9
Unknown	0.2	0.0	0.0	0.0	0.0

(Reaction condition; temperature: 380°C, pressure: 1 atm, contact time: 25 g.h/mol, flow rate of N_2 carrier gas: 60 mL/min)

1.6 Ethanol conversion over Zn-cLDHs catalyst

Table C6 The ethanol conversion and yield of products over Zn-cLDHs catalyst

Time on steam (min)	**60**	**120**	**180**	**240**	**300**	**360**
Conversion (%)	53.0	49.5	49.1	49.2	51.4	47.8
Yield of product (%)						
Ethylene	31.7	30.0	29.8	30.3	32.0	28.8
Diethyl ether	0.4	0.4	0.4	0.4	0.3	0.4
Acetaldehyde	7.4	6.6	6.6	6.3	6.2	6.5
Acetone	1.0	0.9	0.9	0.8	0.9	0.8
Butanal	1.5	1.3	1.2	1.2	1.3	1.2
Diethyl acetal	0.4	0.3	0.3	0.3	0.3	0.3
Isobutylaldehyde dimethyl acetal	0.2	0.0	0.0	0.0	0.2	0.0
C4 alcohols	8.2	8.1	8.1	8.0	8.3	8.0
C6 alcohols	1.3	1.2	1.1	1.0	1.1	1.0
C7 alcohols	0.4	0.3	0.3	0.3	0.3	0.3
C8 alcohols	0.0	0.0	0.0	0.0	0.0	0.0
Aromatic alcohols	0.0	0.0	0.0	0.0	0.0	0.0
C5 carbonyls	0.0	0.0	0.0	0.0	0.0	0.0
C6 carbonyls	0.1	0.0	0.0	0.0	0.0	0.0
C7 carbonyls	0.5	0.4	0.4	0.5	0.5	0.5
C8 carbonyls	0.0	0.0	0.0	0.0	0.0	0.0
C9 carbonyls	0.0	0.0	0.0	0.0	0.0	0.0
Aromatic carbonyls	0.0	0.0	0.0	0.0	0.0	0.0
Unknown	0.0	0.0	0.0	0.0	0.0	0.0

(Reaction condition; temperature: 380°C, pressure: 1 atm, contact time: 25 g.h/mol, flow rate of N_2 *carrier gas: 60 mL/min)*

1.7 Ethanol conversion over Cu-cLDHs catalyst

Table C7 The ethanol conversion and yield of products over Cu-cLDHs catalyst

Time on stream (min)	60	120	180	240	300	360
Conversion (%)	47.3	39.6	42.0	36.1	41.1	43.2
Yield of product (%)						
Ethylene	20.5	18.0	20.1	19.6	21.9	23.8
Diethyl ether	0.0	0.0	0.0	0.0	0.0	0.0
Acetaldehyde	11.2	9.7	10.0	7.7	9.6	9.8
Acetone	0.7	0.6	0.6	0.6	0.6	0.6
Butanal	1.9	1.6	1.5	1.4	1.4	1.5
Diethyl acetal	0.4	0.3	0.3	0.3	0.3	0.4
Isobutylaldehyde dimethyl acetal	0.0	0.0	0.0	0.0	0.0	0.0
C4 alcohols	7.3	6.1	6.7	5.5	6.3	6.0
C6 alcohols	0.8	0.5	0.5	0.4	0.4	0.4
C7 alcohols	1.2	0.8	0.8	0.6	0.7	0.7
C8 alcoholss	0.7	0.4	0.2	0.0	0.0	0.0
Aromatic alcohols	0.4	0.2	0.2	0.0	0.0	0.0
C5 carbonyls	0.0	0.0	0.0	0.0	0.0	0.0
C6 carbonyls	0.0	0.0	0.0	0.0	0.0	0.0
C7 carbonyls	0.4	0.6	0.7	0.0	0.0	0.0
C8 carbonyls	0.4	0.2	0.0	0.0	0.0	0.0
C9 carbonyls	0.2	0.2	0.2	0.0	0.0	0.0
Aromatic carbonyls	1.2	0.5	0.2	0.0	0.0	0.0
Unknown	0.0	0.0	0.0	0.0	0.0	0.0

(Reaction condition; temperature: 380°C, pressure: 1 atm, contact time: 25 g.h/mol, flow rate of N_2 carrier gas: 60 mL/min)

1.8 Ethanol conversion over 4 wt.% Cu-0.8 wt.% Zn/cLDHs catalyst (non-reduced)

Table C8 The ethanol conversion and yield of products over 4 wt.% Cu-0.8 wt.% Zn/cLDHs catalyst

Time on stream (min)	30	60	90	120
Conversion (%)	79.4	79.7	71.0	75.8
Yield of product (%)				
Ethylene	12.4	13.7	10.3	12.4
Diethyl ether	1.3	0.0	1.6	1.8
Acetaldehyde	13.4	12.9	12.7	14.1
Acetone	0.8	0.7	0.6	0.7
Butanal	4.8	4.6	4.3	4.9
Diethyl acetal	1.0	1.0	0.9	1.0
Isobutylaldehyde dimethyl acetal	2.4	2.4	1.0	2.3
C4 alcohols	8.5	8.0	9.3	8.4
C6 alcohols	3.8	3.2	3.4	3.0
C7 alcohols	2.5	2.4	1.9	2.4
C8 alcohols	6.4	6.1	4.5	4.4
Aromatic alcohols	0.2	0.6	1.7	1.2
C5 carbonyls	2.4	2.3	1.1	2.2
C6 carbonyls	1.3	1.3	1.1	1.2
C7 carbonyls	2.3	2.2	1.7	1.9
C8 carbonyls	3.6	3.1	3.0	2.8
C9 carbonyls	2.5	2.1	1.7	1.7
Aromatic carbonyls	8.9	12.4	9.8	8.6
Unknown	0.9	0.7	0.5	0.6

(Reaction condition; temperature: 380°C, pressure: 1 atm, contact time: 25 g.h/mol, flow rate of N_2 carrier gas: 60 mL/min)

1.9 Ethanol conversion over 4 wt.% Cu-0.8 wt.% Zn alloy/cLDHs catalyst (reduced)

Table C9 The ethanol conversion and yield of products over 4 wt.% Cu-0.8 wt.% Zn alloy/cLDHs catalyst (reduced)

Time on stream (min)	**60**	**120**	**180**	**240**	**300**	**360**
Conversion (%)	78.1	76.1	75.1	81.9	83.3	80.8
Yield of product (%)						
Ethylene	15	13.5	14.2	15.9	15.2	13.5
Diethyl ether	0.0	1.7	1.6	1.2	0	0
Acetaldehyde	11.2	14.2	13.7	12.8	11.5	10.5
Acetone	0.8	0.7	0.7	1.8	1.8	1.6
Butanal	4.4	4.2	4	4.3	3.9	4
Diethyl acetal	0.4	0.7	0.7	0.7	1	1
Isobutylaldehyde dimethyl acetal	1.1	1.2	1	2.4	2.4	2.2
C4 alcohols	8	7.8	8.7	7.4	7.7	9.1
C6 alcohols	3.3	2.7	4	3.8	4.3	5.1
C7 alcohols	1.8	1.8	1.8	2.2	2.1	1.9
C8 alcoholss	6	7.7	5.9	6.6	7.1	6.1
Aromatic alcohols	0.4	1	1.6	0.6	1.1	1.1
C5 carbonyls	1.1	1	0.9	2.2	2.4	2.4
C6 carbonyls	0.8	1	1	1.4	1.3	1.4
C7 carbonyls	2.2	2.2	1.4	2.8	2.9	2.7
C8 carbonyls	3	3.1	3.2	3.9	4.2	4.4
C9 carbonyls	1.9	1.9	1.7	2.4	2.6	2.5
Aromatic carbonyls	11.1	9.7	9.7	10.5	11.8	10.7
Unknown	0.6	0.5	0.5	1	1.1	1.1

(Reaction condition; temperature: 380°C, pressure: 1 atm, contact time: 25 g.h/mol, flow rate of N_2 carrier gas: 60 mL/min)

1.10 Ethanol conversion over 10 wt.% Cu-2 wt.% Zn/cLDHs catalyst (non-reduced)

Table C10 The ethanol conversion and yield of products over 10 wt.% Cu-2 wt.% Zn/cLDHs catalyst

Time on stream (min)	**60**	**120**	**180**	**240**	**300**	**360**
Conversion (%)	78.1	82.3	77.8	75.1	84.0	72.4
Yield of product (%)						
Ethylene	12.2	8.4	9.1	10.1	8.7	9.7
Diethyl ether	2.5	1.7	2.0	2.0	1.4	1.8
Acetaldehyde	18.4	13.7	15.8	16.7	13.6	16.8
Acetone	0.9	0.6	0.6	0.6	0.6	0.6
Butanal	7.2	5.0	5.3	5.4	5.0	5.2
Diethyl acetal	0.3	1.0	1.0	1.0	1.1	1.0
Isobutylaldehyde dimethyl acetal	2.8	2.1	2.1	2.1	2.4	1.1
C4 alcohols	6.7	8.0	8.1	8.0	8.3	7.6
C6 alcohols	2.0	4.2	3.5	2.8	5.5	2.7
C7 alcohols	1.9	1.6	2.2	2.2	3.2	1.3
C8 alcoholss	3.9	9.2	5.2	5.5	6.5	4.1
Aromatic alcohols	1.0	0.4	0.6	0.9	0.7	2.3
C5 carbonyls	2.3	2.1	2.0	1.9	2.3	1.9
C6 carbonyls	1.3	1.6	1.5	1.3	1.8	1.1
C7 carbonyls	1.8	2.7	2.1	1.8	2.2	1.3
C8 carbonyls	2.1	4.6	3.8	2.6	6.2	1.8
C9 carbonyls	1.1	2.4	1.8	1.4	3.4	1.8
Aromatic carbonyls	9.2	11.8	10.1	8.2	9.6	9.5
Unknown	0.5	1.2	0.9	0.7	1.5	0.6

(Reaction condition; temperature: 380°C, pressure: 1 atm, contact time: 25 g.h/mol, flow rate of N_2 carrier gas: 60 mL/min)

1.11 Ethanol conversion over 10 wt.% Cu-2 wt.% Zn alloy/cLDHs catalyst (reduced)

Table C11 The ethanol conversion and yield of products over 10 wt.% Cu-2 wt.% Zn alloy/cLDHs catalyst (reduced)

Time on stream (min)	**60**	**120**	**180**	**240**	**300**
Conversion (%)	67.8	87	76.7	75.3	78
Yield of product (%)					
Ethylene	13.5	19.8	14.2	15.1	15
Diethyl ether	2.1	0.0	1.8	1.5	2.2
Acetaldehyde	21.2	18.2	21.7	20.3	26.5
Acetone	0.8	2.9	0.9	1.0	0.8
Butanal	6.2	6.2	5.7	6.3	5.1
Diethyl acetal	1.2	1.4	1.1	1.2	1.1
Isobutylaldehyde dimethyl acetal	1.1	2.9	2.2	2.4	2.1
C4 alcohols	5.8	6.9	6.1	6.7	6.2
C6 alcohols	0.9	2.0	1.6	1.9	1.6
C7 alcohols	2.6	4.1	3.4	3.9	3.6
C8 alcohols	1.8	2.6	2.0	1.6	1.7
Aromatic alcohols	1.2	1.5	1.8	0.9	0.4
C5 carbonyls	0.9	2.4	1.7	2.0	1.7
C6 carbonyls	0.8	1.3	0.9	1.1	0.8
C7 carbonyls	0.7	1.9	1.3	1.0	1.0
C8 carbonyls	1.2	1.9	1.4	1.0	1.2
C9 carbonyls	0.9	1.2	0.7	0.7	0.7
Aromatic carbonyls	4.8	9.2	7.5	6.6	6.2
Unknown	0.2	0.5	0.6	0.2	0.2

(Reaction condition; temperature: 380°C, pressure: 1 atm, contact time: 25 g.h/mol, flow rate of N_2 *carrier gas: 60 mL/min)*

1.12 Ethanol conversion over 1 wt.% Ru/cLDHs catalyst (non-reduced)

Table C12 The ethanol conversion and yield of products over 1 wt.% Ru/cLDHs catalyst (non-reduced)

Time on stream (min)	**60**	**120**	**180**	**240**	**300**	**360**
Conversion (%)	56.3	59.1	52.0	49.2	51.6	49.9
Yield of product (%)						
Ethylene	14.1	16.6	15.8	17.9	19.3	18.9
Diethyl ether	1.9	1.7	1.7	1.8	1.9	2.0
Acetaldehyde	9.2	8.8	8.8	9.1	8.9	9.1
Acetone	1.1	1.0	0.6	0.6	1.0	0.6
Butanal	2.2	2.2	2.0	2.0	2.1	2.0
Diethyl acetal	0.5	0.5	0.5	0.5	0.5	0.5
Isobutylaldehyde dimethyl acetal	0.6	0.8	0.8	0.6	0.7	0.7
C4 alcohols	11.3	10.5	10.8	10.5	10.3	10.1
C6 alcohols	3.3	3.4	2.6	2.1	2.2	2.0
C7 alcohols	0.8	0.8	0.6	0.5	0.6	0.5
C8 alcohols	3.3	3.6	1.7	0.7	0.6	0.6
Aromatic alcohols	0.4	0.4	0.2	0.2	0.2	0.0
C5 carbonyls	0.8	0.7	0.7	0.7	0.5	0.6
C6 carbonyls	0.5	0.6	0.5	0.2	0.4	0.4
C7 carbonyls	1.2	1.4	0.8	0.6	0.8	0.6
C8 carbonyls	1.0	1.1	0.7	0.2	0.3	0.2
C9 carbonyls	0.6	0.7	0.4	0.2	0.2	0.0
Aromatic carbonyls	3.4	4.2	2.9	0.8	1.1	1.0
Unknown	0.0	0.0	0.0	0.0	0.0	0.0

(Reaction condition; temperature: 380°C, pressure: 1 atm, contact time: 25 g.h/mol, flow rate of N_2 carrier gas: 60 mL/min)

1.13 Ethanol conversion over 1 wt.% Ru/cLDHs catalyst (reduced)

Table C13 The ethanol conversion and yield of products over 1 wt.% Ru/cLDHs catalyst (reduced)

Time on stream (min)	60	120	180	240	300	360
Conversion (%)	71.6	51.2	48.0	67.2	56	52.9
Yield of product (%)						
Ethylene	29.7	16.9	17.2	28.3	22.5	21.7
Diethyl ether	0.2	2.0	1.7	0.3	0.3	0.4
Acetaldehyde	9.8	10.1	9.0	9.6	8.8	9.2
Acetone	2.1	0.6	0.5	1.8	1.1	0.6
Butanal	2.9	2.5	2.1	2.9	2.4	2.2
Diethyl acetal	1.0	0.7	0.6	0.8	0.7	0.6
Isobutylaldehyde dimethyl acetal	3.4	0.8	0.6	3.1	0.9	0.8
C4 alcohols	8.8	10	9.7	8.7	9.5	9.2
C6 alcohols	2.2	2.2	2.3	2.4	2.7	2.2
C7 alcohols	1.0	0.7	0.6	0.9	0.7	0.6
C8 alcohols	2.1	0.5	0.8	1.5	1.6	1.0
Aromatic alcohols	0.0	0.0	0.2	0.0	0.0	0.2
C5 carbonyls	2.2	0.6	0.3	1.7	0.4	0.4
C6 carbonyls	0.8	0.5	0.4	0.7	0.5	0.4
C7 carbonyls	1.8	0.9	0.5	1.6	1.0	0.8
C8 carbonyls	1.0	0.9	0.6	1.0	1.1	0.8
C9 carbonyls	0.6	0.3	0	0.5	0.5	0.2
Aromatic carbonyls	1.8	0.8	0.9	1.5	1.5	1.7
Unknown	0.0	0.0	0.0	0.0	0.0	0.0

(Reaction condition; temperature: 380°C, pressure: 1 atm, contact time: 25 g.h/mol, flow rate of N_2 carrier gas: 60 mL/min)

2. Conversion of ethanol to higher alcohols over cLDHs

2.1 Effect of contact time time over cLDHs(3) catalyst

Table C14 The ethanol conversion and yield of products and contact time 15 g.h/mol

Time on stream (min)	**60**	**120**	**180**	**240**	**300**	**360**
Conversion (%)	37.9	33.1	32.9	27.1	28.7	32.1
Yield of product (%)						
Ethylene	18.9	15.6	16.8	13.0	14.6	17.6
Diethyl ether	3.3	3.1	3.0	3.0	3.0	2.8
Acetaldehyde	6.2	5.7	5.6	5.2	5.2	5.7
Acetone	0.5	0.4	0.2	0.0	0.0	0.2
Butanal	1.0	0.9	0.8	0.6	0.6	0.8
Diethyl acetal	0.3	0.2	0.2	0.0	0.0	0.2
Isobutylaldehyde dimethyl acetal	0.2	0.2	0.2	0.0	0.0	0.0
C4 alcohols	6.9	6.5	5.7	5.0	5.0	4.3
C6 alcohols	0.6	0.5	0.5	0.3	0.3	0.3
C7 alcohols	0.0	0.0	0.0	0.0	0.0	0.0
C8 alcohols	0.0	0.0	0.0	0.0	0.0	0.0
Aromatic alcohols	0.0	0.0	0.0	0.0	0.0	0.0
C5 carbonyls	0.0	0.0	0.0	0.0	0.0	0.2
C6 carbonyls	0.0	0.0	0.0	0.0	0.0	0.0
C7 carbonyls	0.0	0.0	0.0	0.0	0.0	0.0
C8 carbonyls	0.0	0.0	0.0	0.0	0.0	0.0
C9 carbonyls	0.0	0.0	0.0	0.0	0.0	0.0
Aromatic carbonyls	0.0	0.0	0.0	0.0	0.0	0.0
Unknowns	0.0	0.0	0.0	0.0	0.0	0.0

(Reaction condition; temperature: 380°C, pressure: 1 atm, contact time: 15 g.h/mol, flow rate of N_2 carrier gas: 60 mL/min)

Table C15 The ethanol conversion and yield of products and contact time 30 g.h/mol

Time on stream (min)	**30**	**60**	**90**	**120**	**150**	**180**
Conversion (%)	60.6	59.6	56.3	57.8	57.8	53.4
Yield of product (%)						
Ethylene	26.0	24.9	23.2	25.1	26.7	23.1
Diethyl ether	3.9	4.5	4.3	4.3	3.8	3.5
Acetaldehyde	9.0	9.0	8.7	8.6	8.3	7.8
Acetone	1.2	1.2	1.0	1.1	1.1	0.9
Butanal	2.5	2.4	2.2	2.2	2.1	1.9
Diethyl acetal	0.5	0.5	0.5	0.5	0.5	0.4
Isobutylaldehyde dimethyl acetal	1.0	0.9	0.8	0.9	0.8	0.7
C4 alcohols	10.7	10.7	10.6	10.3	10.1	10.5
C6 alcohols	2.6	2.4	2.2	2.3	2.0	2.3
C7 alcohols	0.4	0.4	0.4	0.4	0.4	0.3
C8 alcohols	0.4	0.4	0.3	0.3	0.3	0.3
Aromatic alcohols	0.0	0.0	0.0	0.0	0.0	0.0
C5 carbonyls	0.5	0.5	0.5	0.5	0.6	0.4
C6 carbonyls	0.6	0.5	0.5	0.5	0.4	0.4
C7 carbonyls	0.9	0.8	0.8	0.8	0.7	0.7
C8 carbonyls	0.6	0.5	0.4	0.2	0.2	0.4
C9 carbonyls	0.0	0.0	0.0	0.0	0.0	0.0
Aromatic carbonyls	0.0	0.0	0.0	0.0	0.0	0.0
Unknowns	0.0	0.0	0.0	0.0	0.0	0.0

(Reaction condition; temperature: 380°C, pressure: 1 atm, contact time: 30 g.h/mol, flow rate of N_2 carrier gas: 60 mL/min)

APPENDIX D

CATALYST CHARACTERIZATION

X-RAY DIFFRACTION PATTERN OF CATALYST

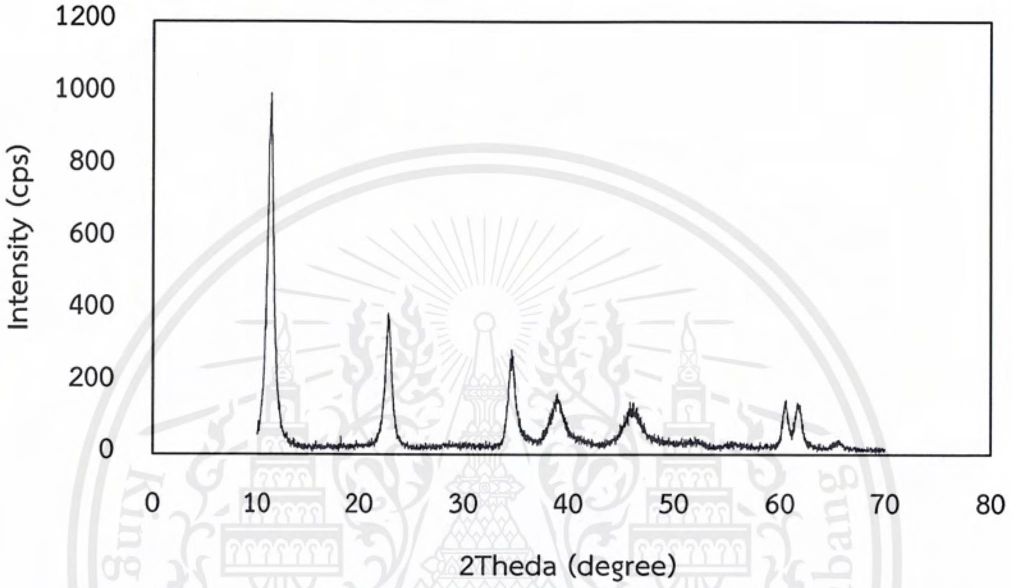

Figure D1 X-ray diffraction pattern of non-calcined LDHs Mg/Al ratio 3:1

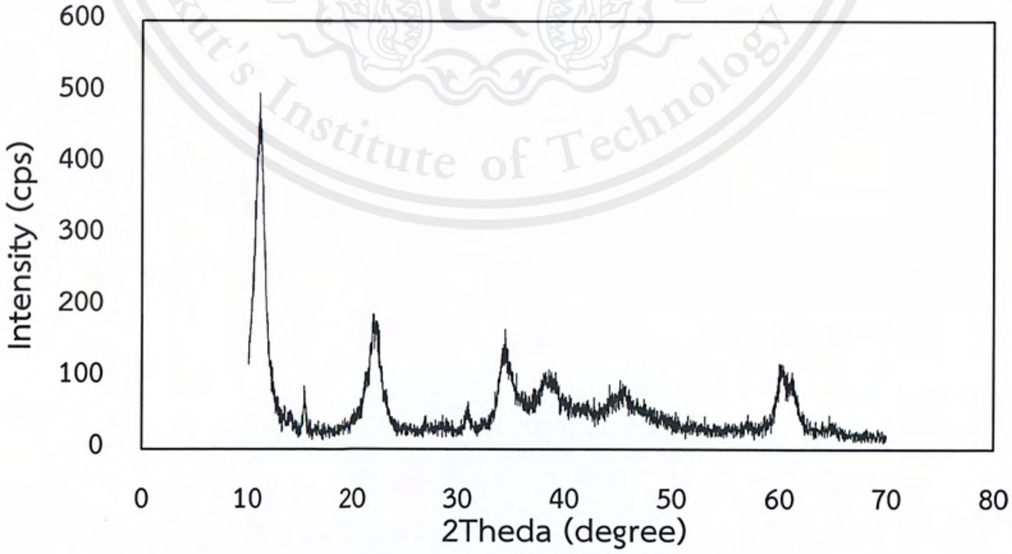

Figure D2 X-ray diffraction pattern of non-calcined Mg/Al LDHs ratio 6:1

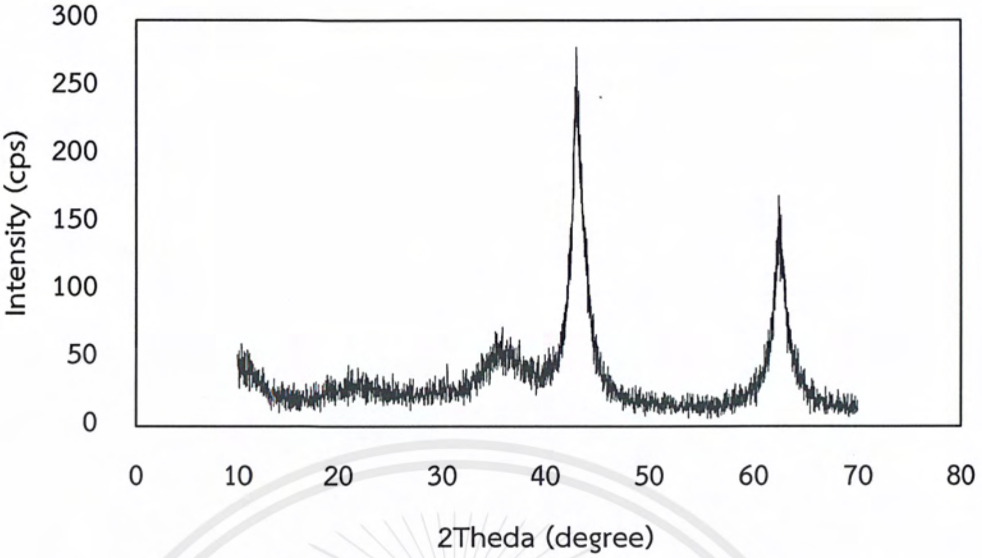

Figure D2 X-ray diffraction pattern of calcined LDHs Mg/Al ratio 3:1

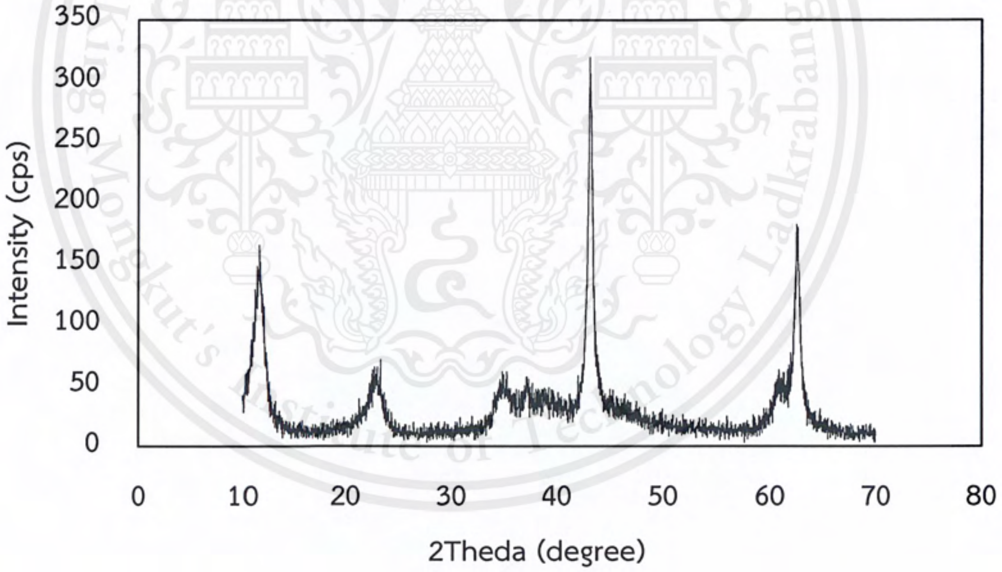

Figure D4 X-ray diffraction pattern of calcined LDHs Mg/Al ratio 6:1

ADSORPTION-DESORPTION ISOTHERM

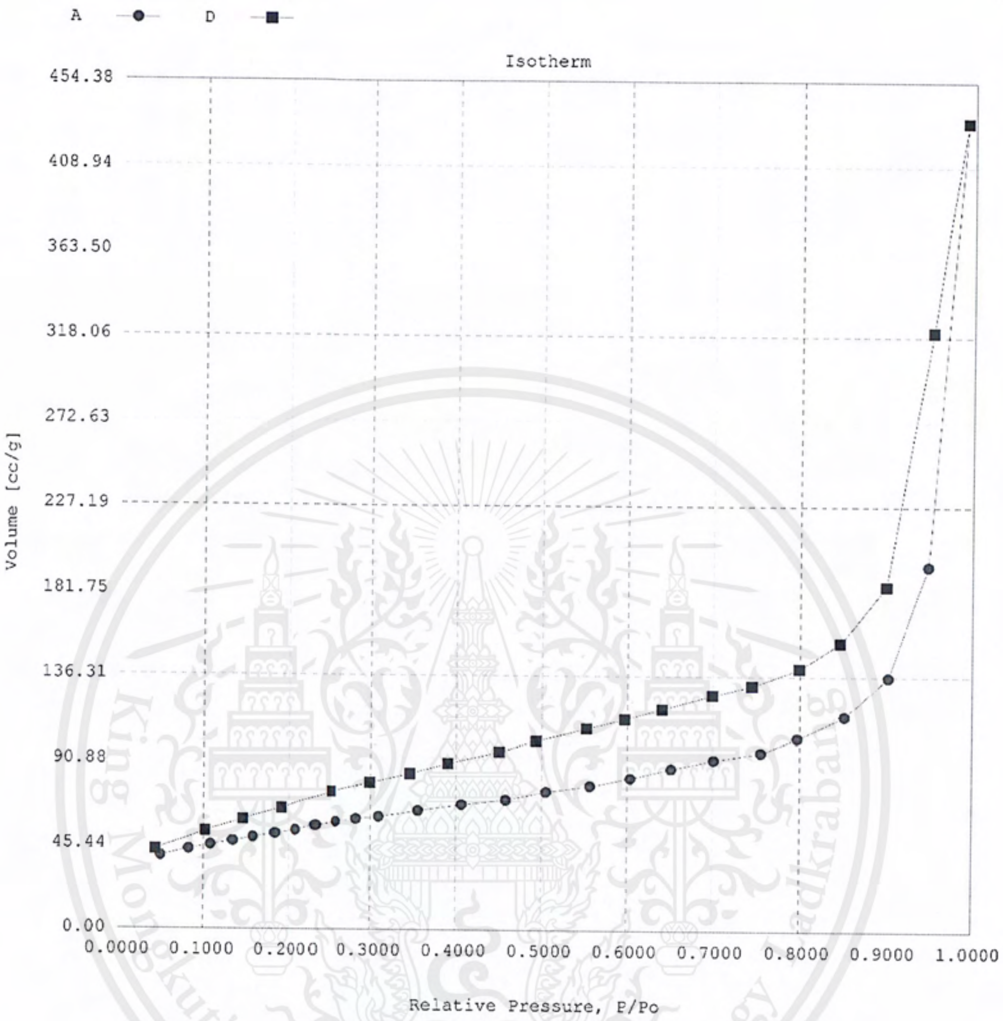

Figure D5 Adsorption-desorption isotherm of cLDHs(1)

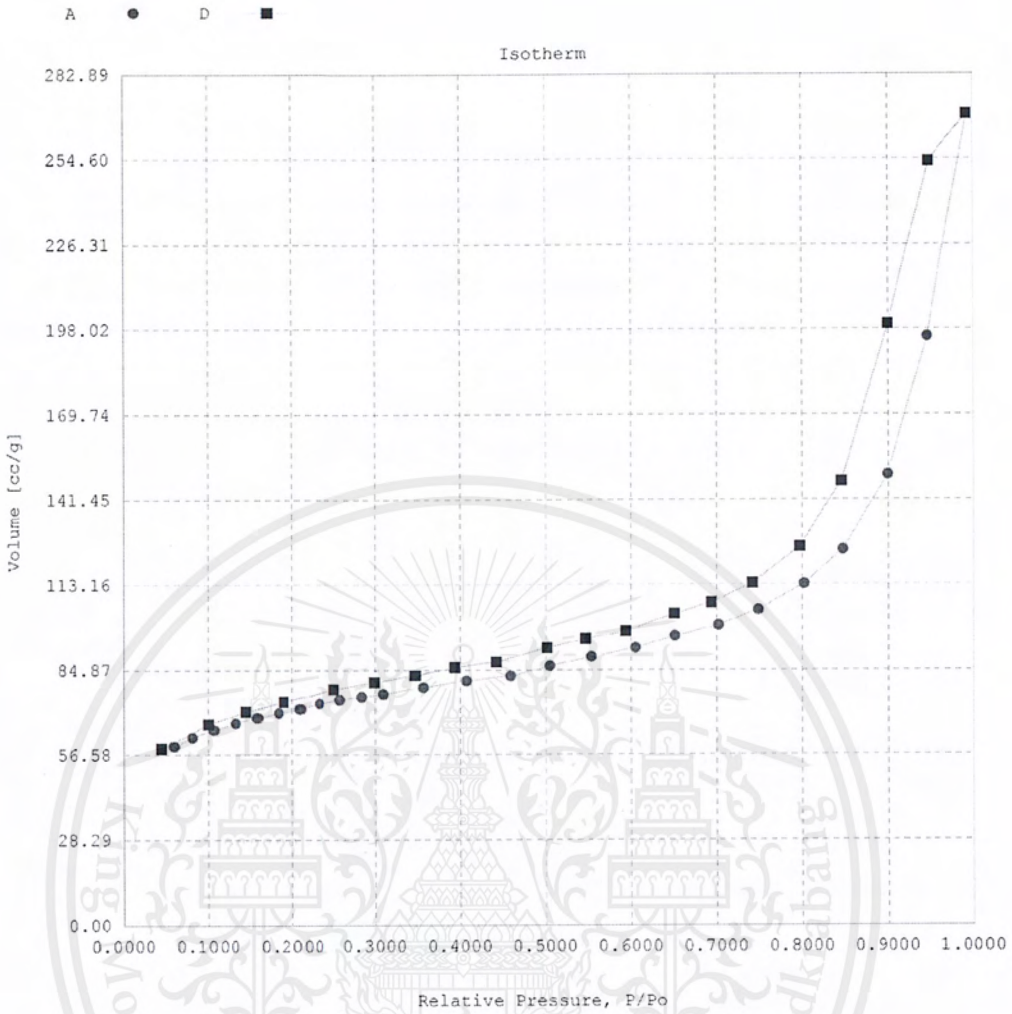

Figure D6 Adsorption-desorption isotherm of cLDHs(2)

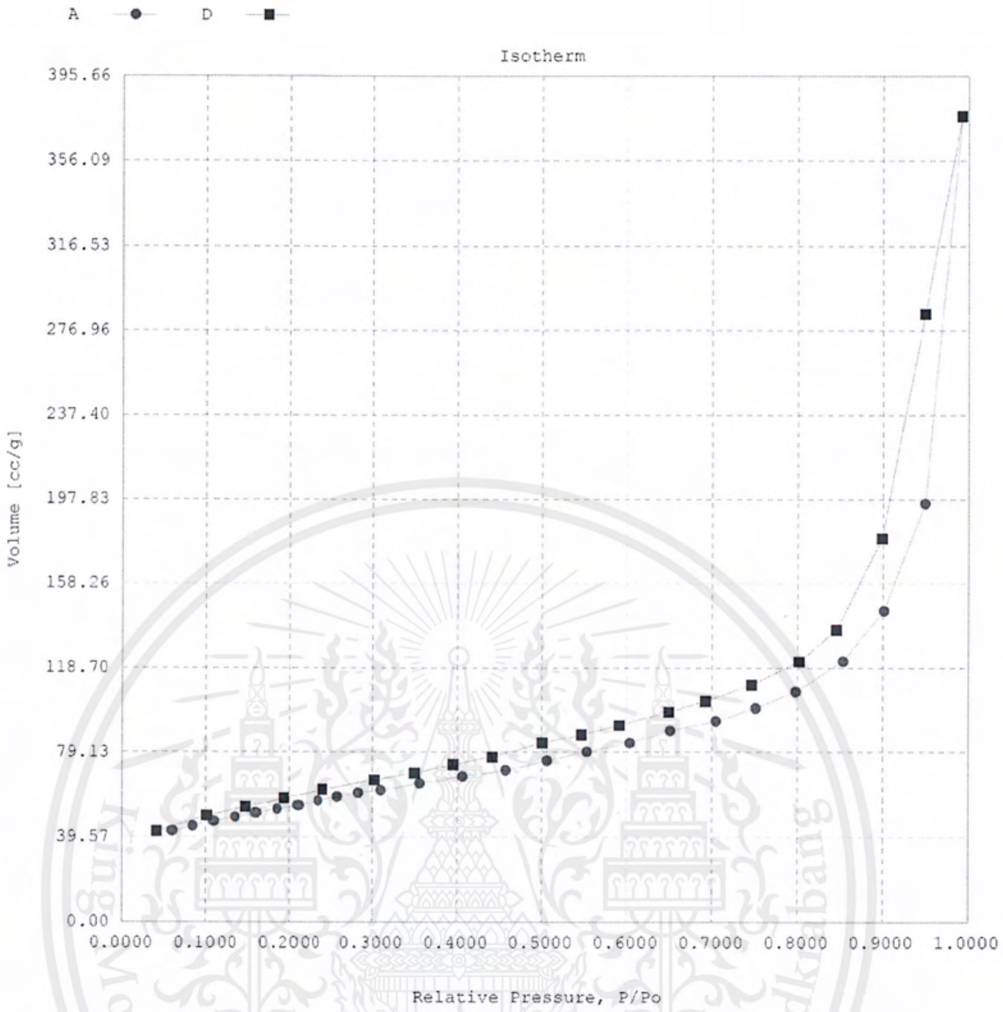

Figure D7 Adsorption-desorption isotherm of cLDHs(3)

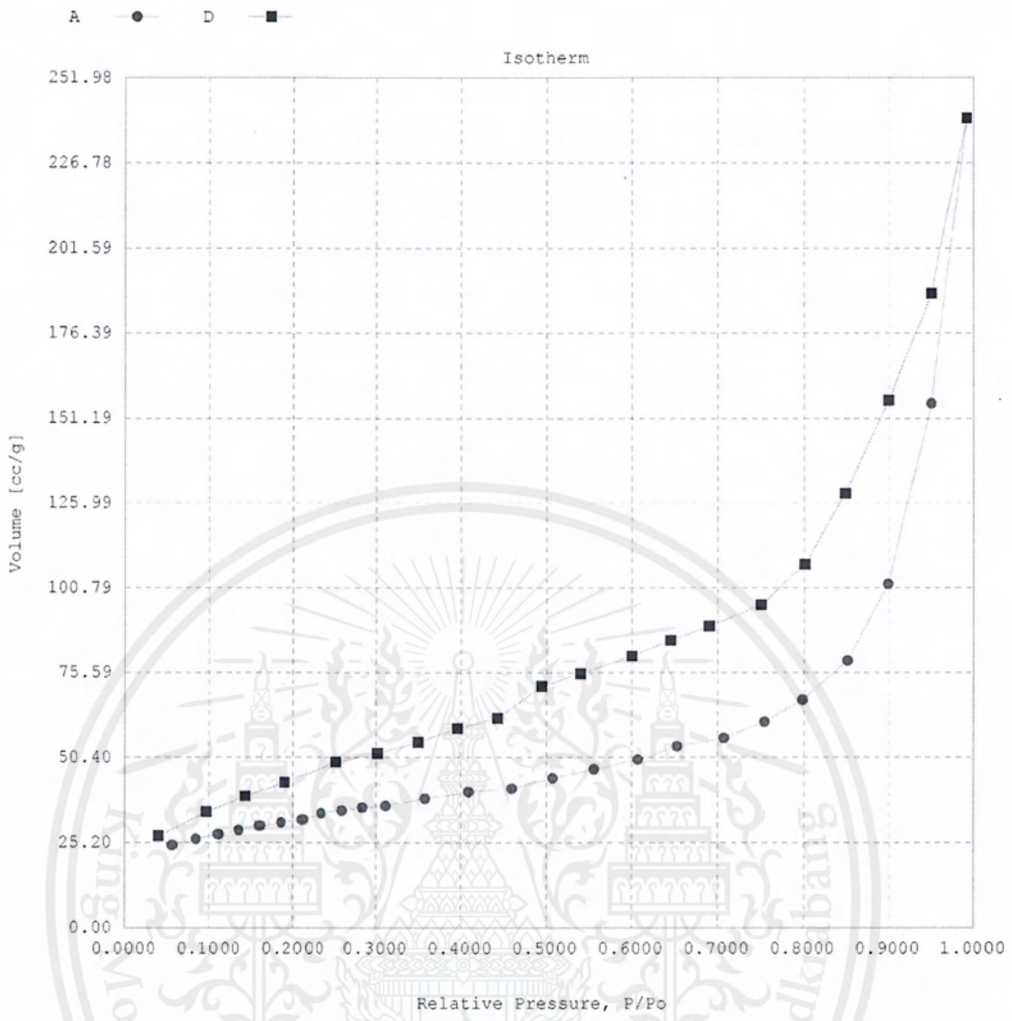

Figure D8 Adsorption-desorption isotherm of cLDHs(6)

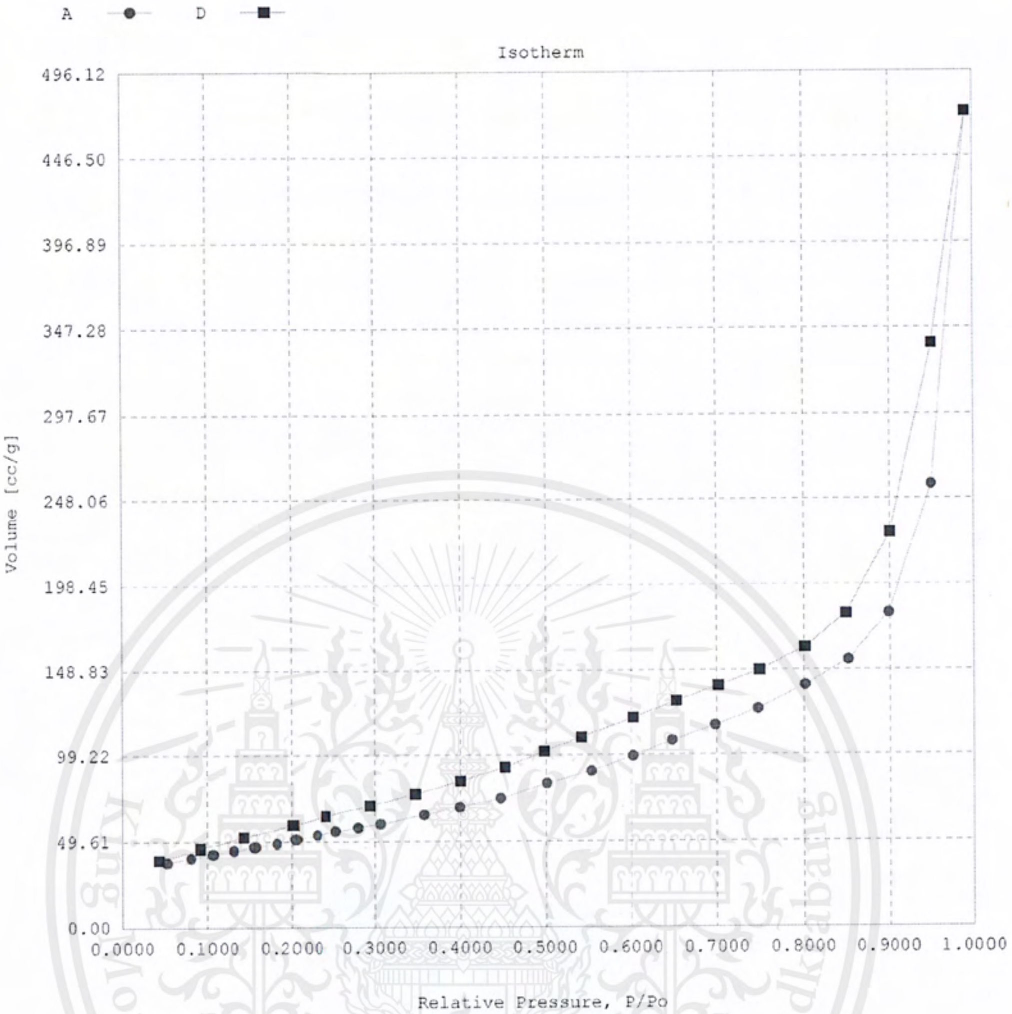

Figure D9 Adsorption-desorption isotherm of Fe-cLDHs

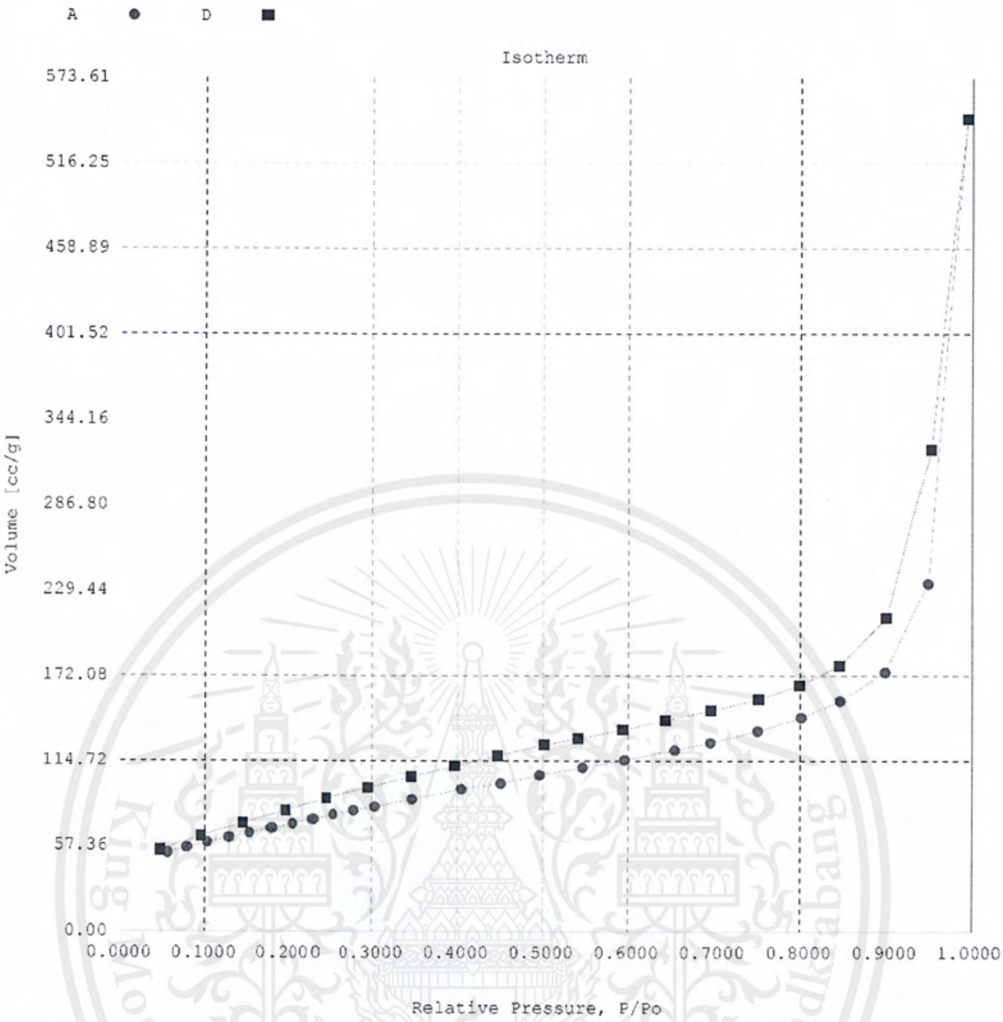

Figure D10 Adsorption-desorption isotherm of Zn-cLDHs

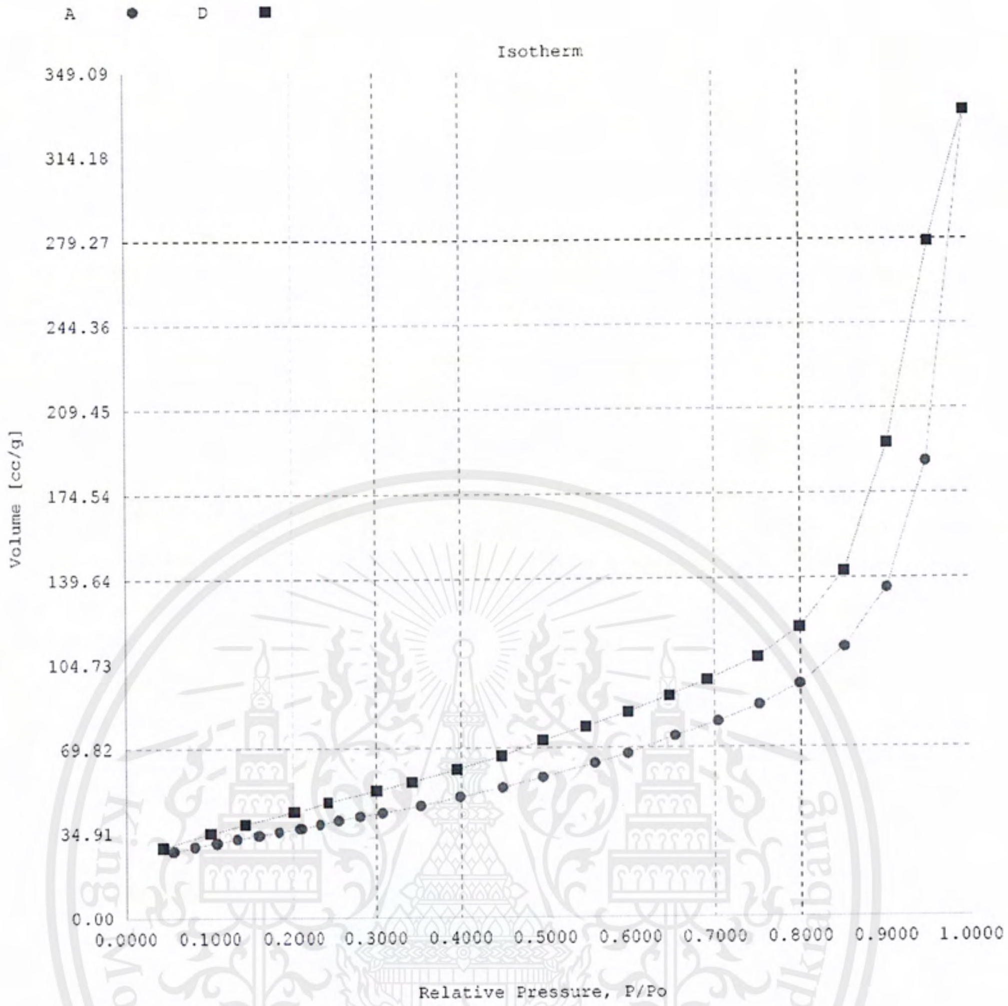

Figure D11 Adsorption-desorption isotherm of Cu-cLDHs

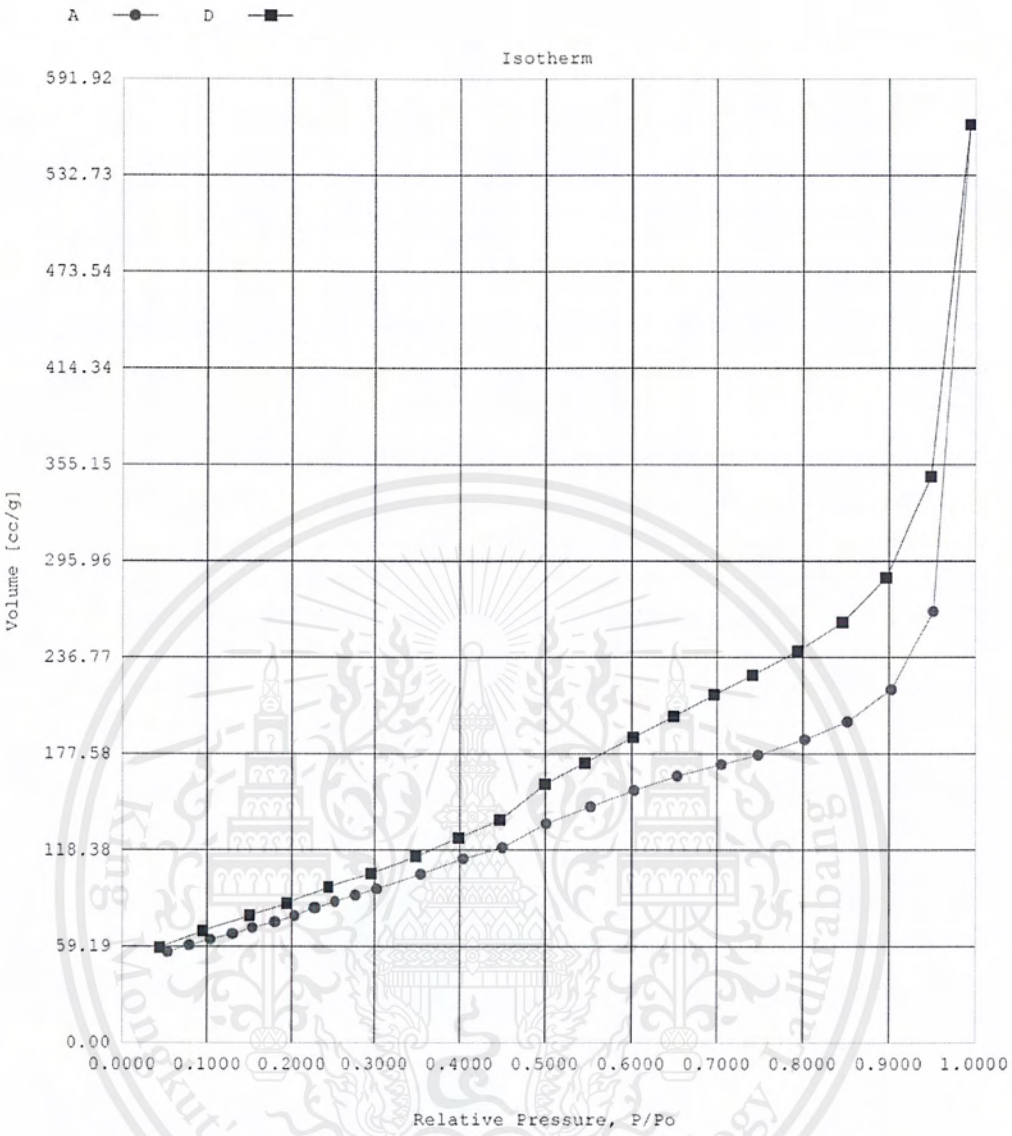

Figure D12 Adsorption-desorption isotherm of 4 wt.% Cu-0.8 wt.% Zn/cLDHs

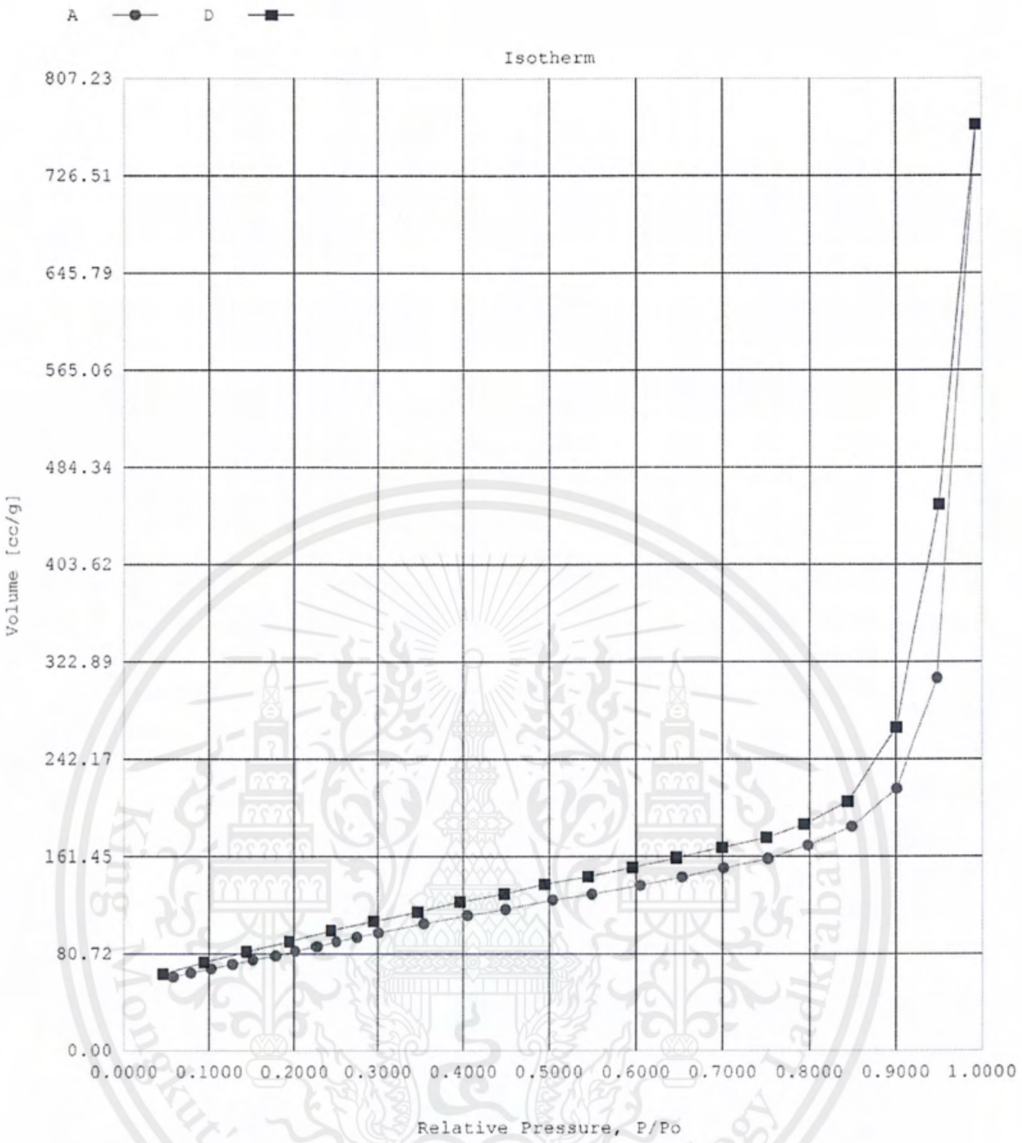

Figure D13 Adsorption-desorption isotherm of cLDHs(3) support of 4 wt.% Cu-0.8 wt.% Zn/cLDHs

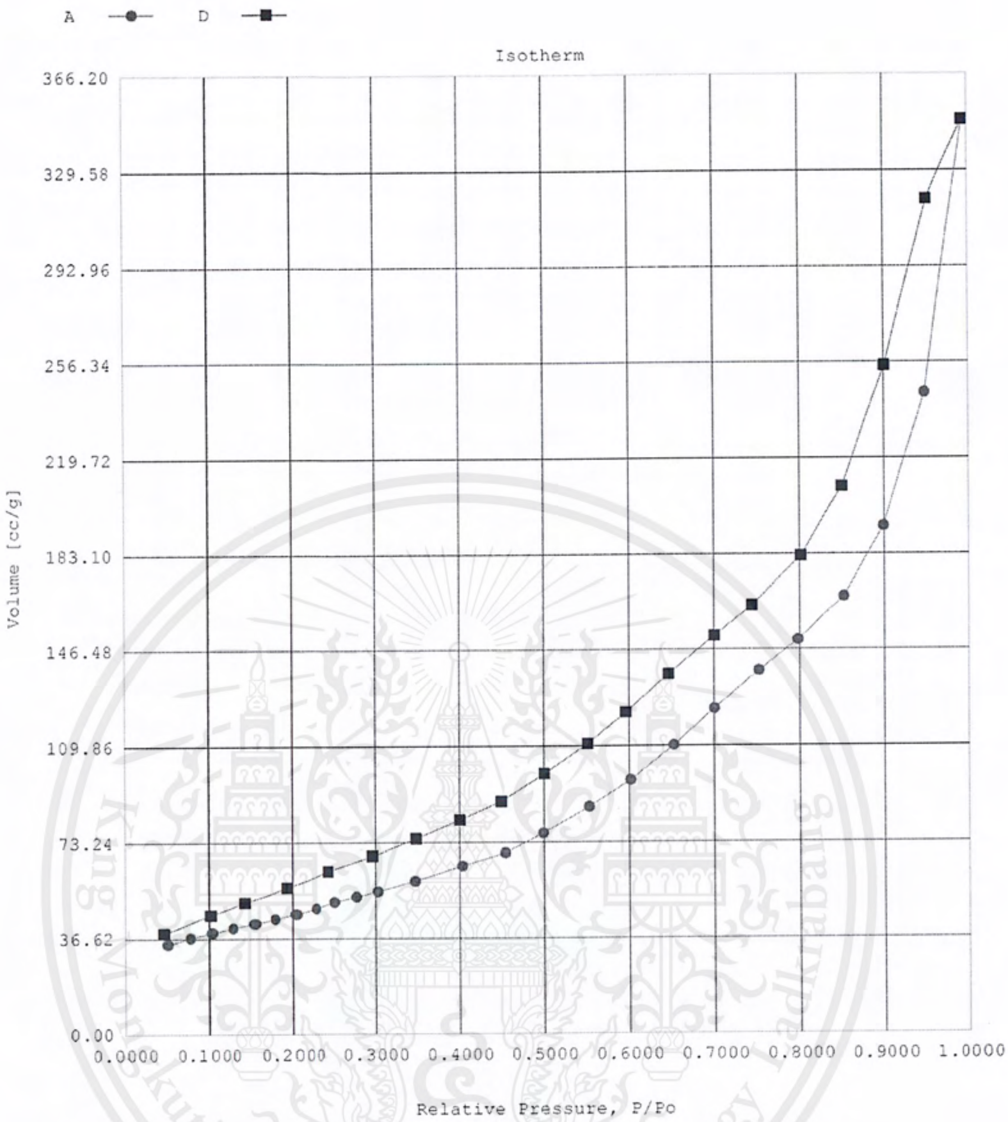

Figure D14 Adsorption-desorption isotherm of 10 wt.% Cu-0.8 wt.% Zn/cLDHs

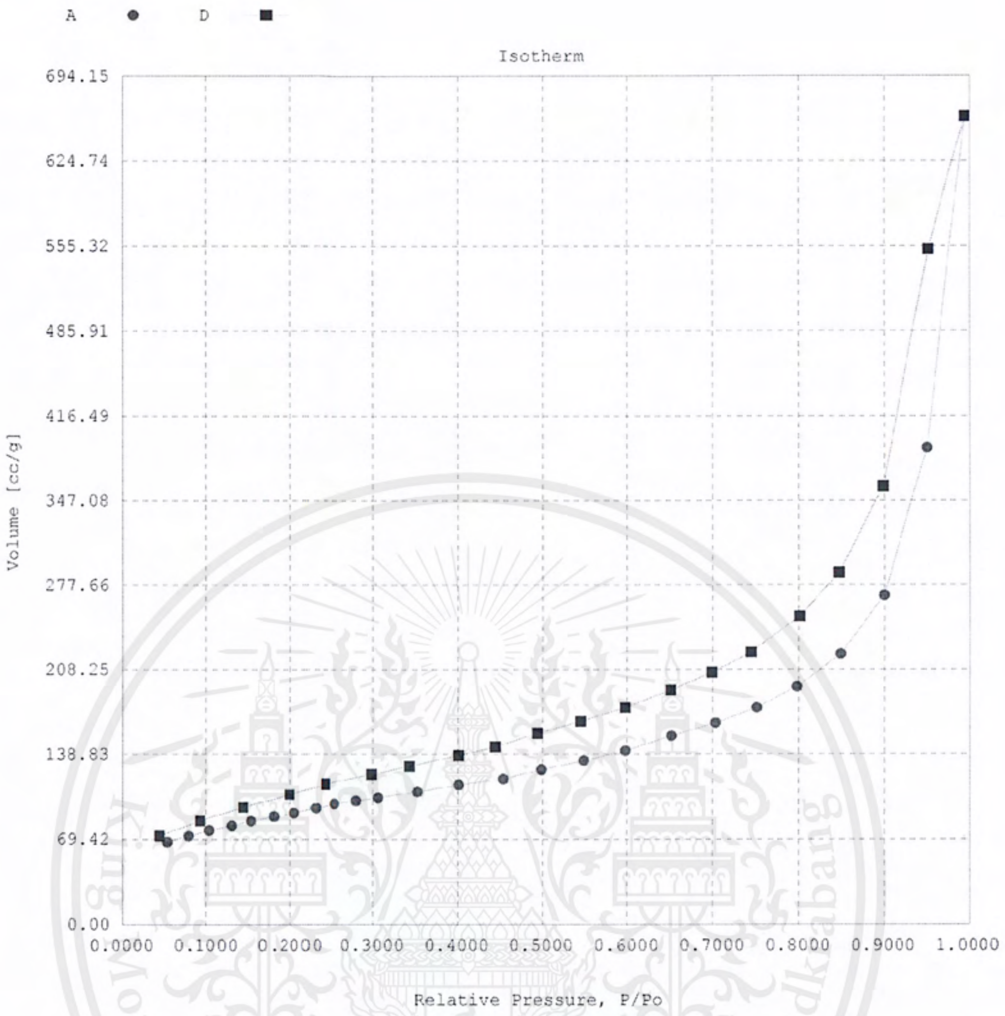

Figure D15 Adsorption-desorption isotherm of 1 wt.% Ru/cLDHs

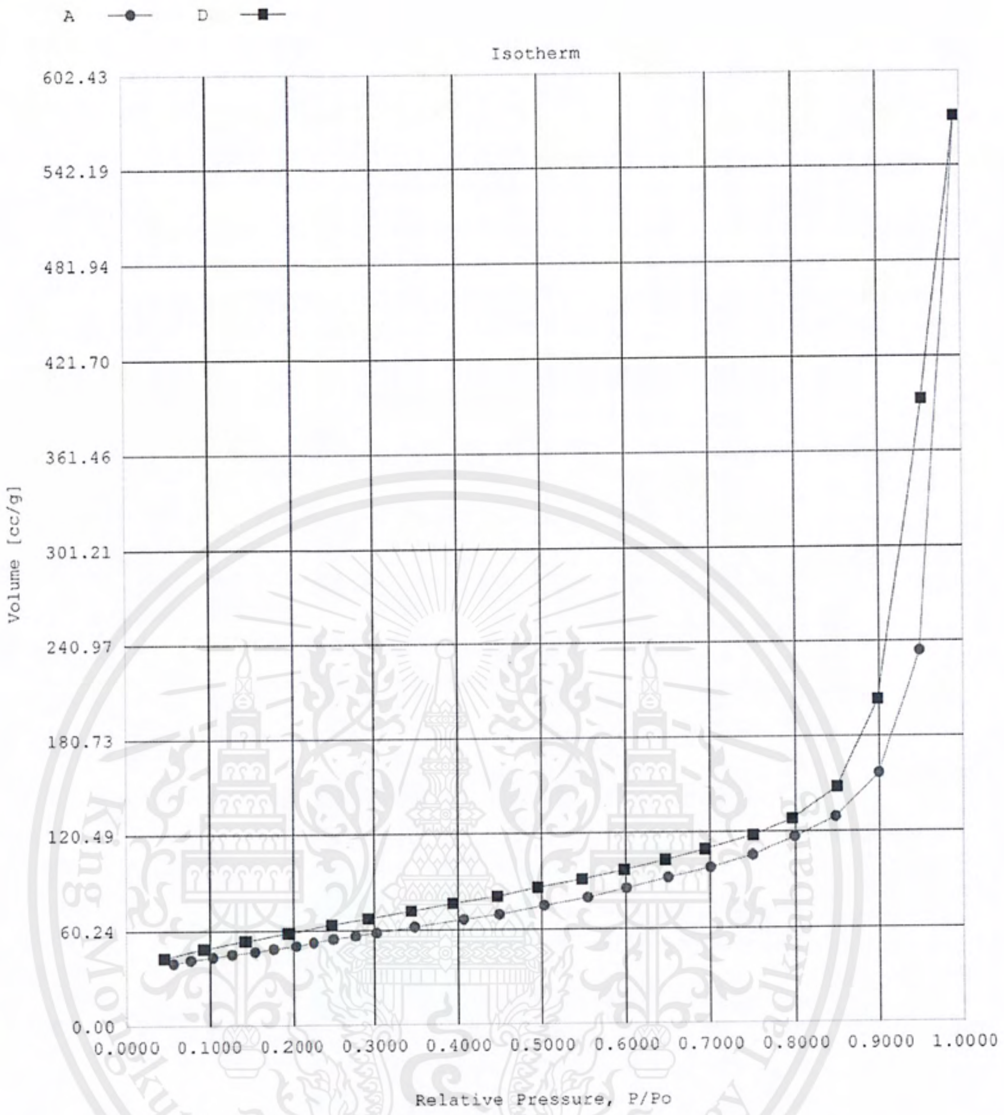

Figure D16 Adsorption-desorption isotherm of support cLDHs support for 1 wt.% Ru adsorption

TEMPERATURE PROGRAMED DESORPTION

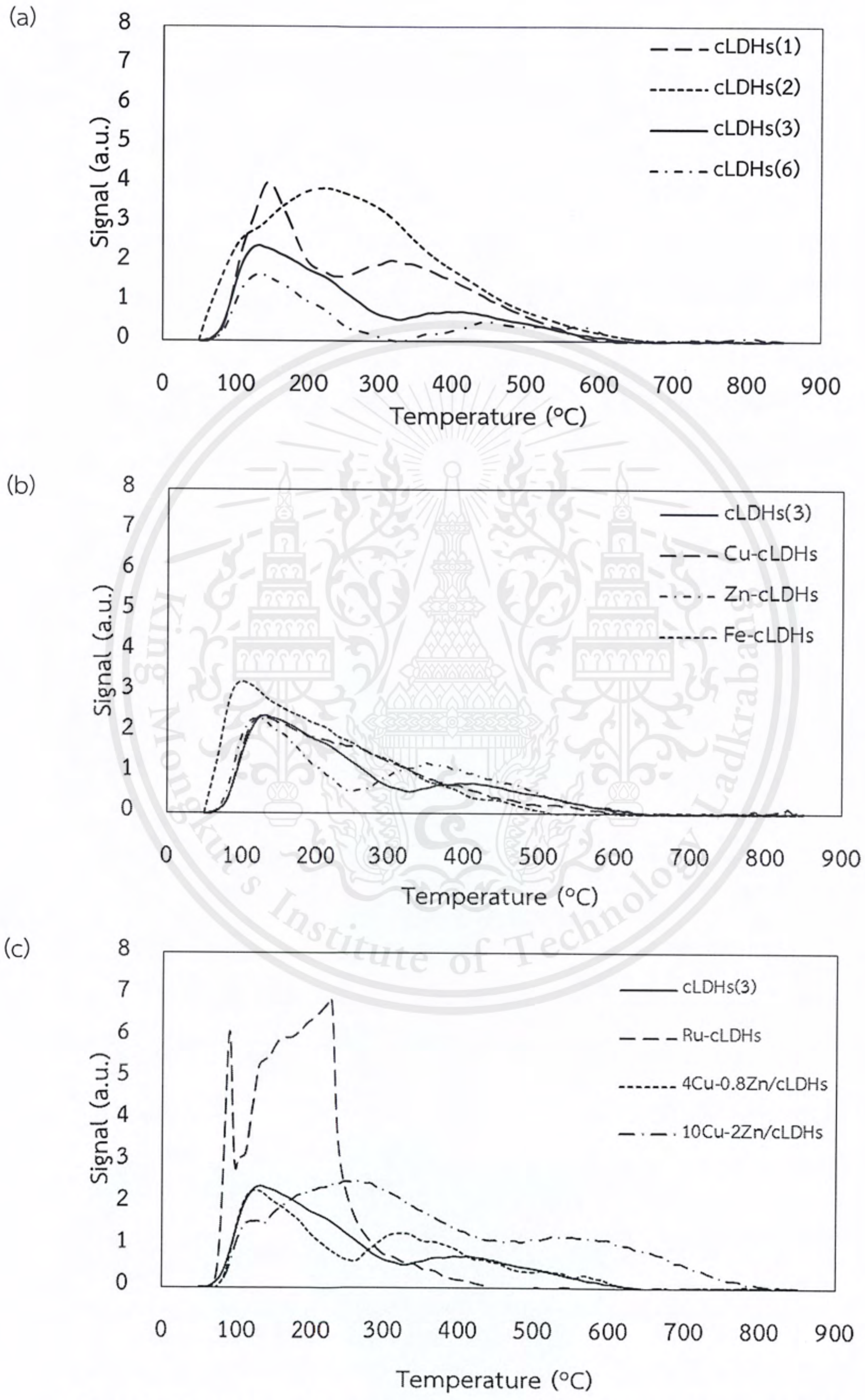

Figure D17 NH_3-temperature programmed desorption profile of catalysts

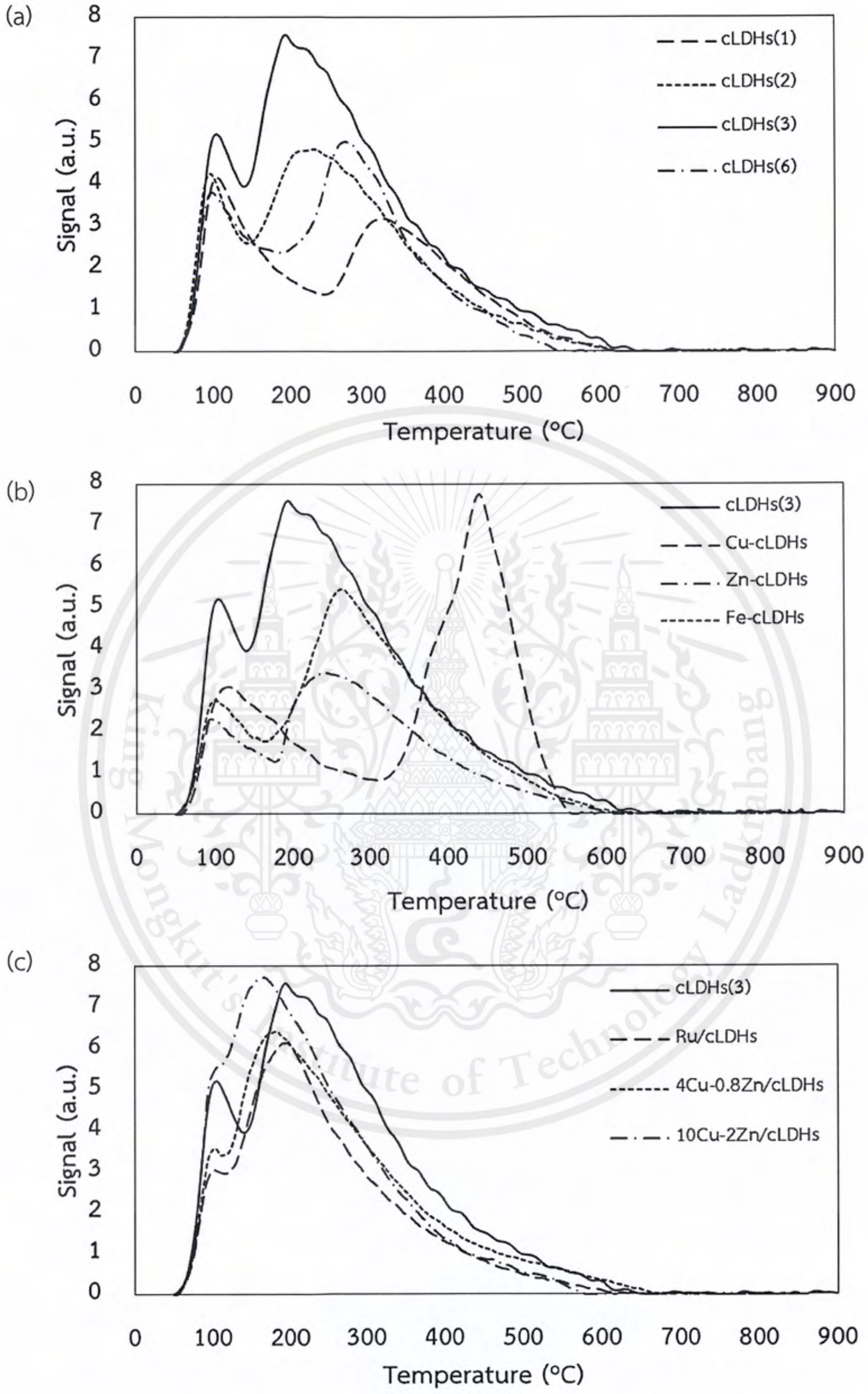

Figure D18 CO_2-temperature programmed desorption profile of catalysts